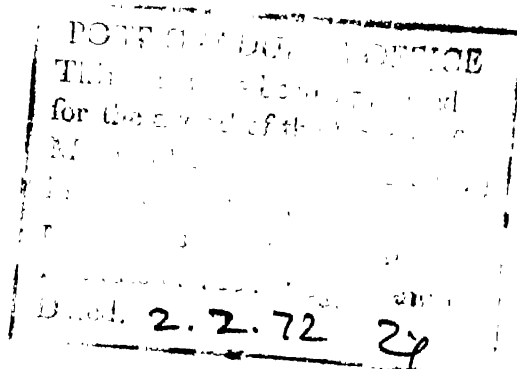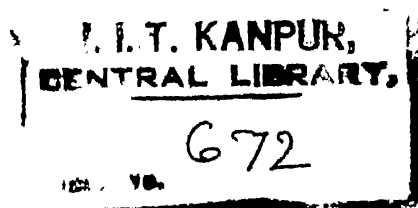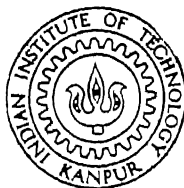# EFFECT OF IMPURITIES
ON
HE STRUCTURE OF IRREGULAR EUTECTIC ALLOYS

A THESIS SUBMITTED

In Partial Fulfilment of the Requirements

for the Degree of
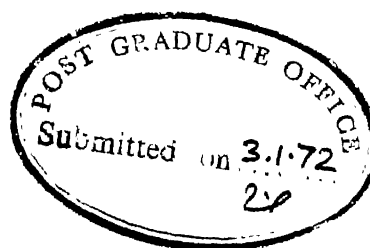
MASTER OF TECHNOLOGY

By

LALIT KUMAR

ME-1972-M-KUM-EFF

DEPARTMENT OF METALLURGICAL ENGINEERING
INDIAN INSTITUTE OF TECHNOLOGY KANPUR
JANUARY 1972

CERTIFICATE

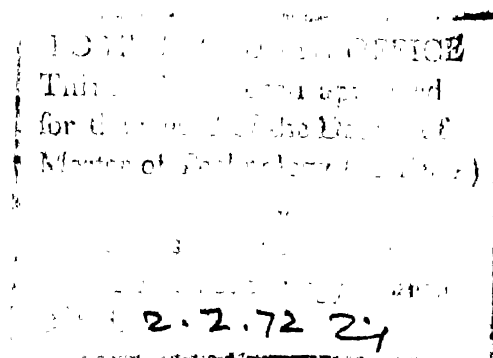Certified that this work on 'Effect of Impurities on the Structure of Irregular Eutectic Alloys' has been carried out under my supervision and that has not been submitted elsewhere for a degree.

H. D. Merchant

(H. D. Merchant)
Visiting Associate Professor
Dept. of Metallurgical Engineering
Indian Institute of Technology,
Kanpur

ACKNOWLEDGEMENTS

LIST OF CONTENTS

LIST OF FIGURES

LIST OF TABLES

SUMMARY

The work consists of three parts, purification of the alloy, directional solidification and study of microstructure. For purification, zone refining with different number of passes was used. Seven alloys of eutectic composition were used for this purpose. Instead of refining the individual components and then making the alloys, the alloys of eutectic composition were zone refined. By doing so the actual amount of work involved was sufficiently reduced, some impurities which were difficult to remove in pure metal could be removed in alloys and any pro-eutectic component present would also segregate on one end, and the middle part of the bar left with eutectic composition.

The purified alloys were grown directionally at a speed of 20 mm/hr. This resulted in orienting the phases in the direction of growth. Three mutually perpendicular sections (transverse, vertical longitudinal and horizontal longitudinal) were taken from the centre of the bar for microstructure study. The most remarkable realignment of the second phase was observed in Bi-Cd, Zn-Sb and Sn-Zn eutectic alloys and alighter alignment in case of Bi-Sn and Bi-Zn alloys. The change in structure is most probably due to slow growth rate, lower impurity content and hence the reduced incidence of twinning.

SUMMARY

The work consists of three parts, purification of the alley, directional solidification and study of microstructure. For purification, zone refining with different number of passes was used. Seven alloys of eutectic composition were used for this purpose. Instead of refining the individual components and then making the alloys, the alloys of eutectic composition were zone refined. By doing so the actual amount of work involved was sufficiently reduced, some impurities which were difficult to remove in pure metal could be removed in alloys and any pro-eutectic component present would also segregate on one end, and the middle part of the bar left with eutectic composition.

The purified alleys were grown directionally at a speed of 20 mm/hr. This resulted in orienting the phases in the direction of growth. Three mutually perpendicular sections (transverse, vertical longitudinal and horizontal longitudinal) were taken from the centre of the bar for microstructure study. The most remarkable realignment of the second phase was observed in Bi-Cd, Zn-Sb and Sn-Zn eutectic alloys and a lighter alignment in case of Bi-Sn and Bi-Zn alloys. The change in structure is most probably due to slow growth rate, lower impurity content and hence the reduced incidence of twinning.

CHAPTER 1

INTRODUCTION

Eutectic alley may be defined as the alloy composition that freezes at a constant temperature, undergoing the eutectic reaction completely. It can also be defined as an alloy composition at which two descending liquidus curves in a binary system, or three descending liquidus surfaces in a ternary system meet at a point. Thus such an alloy has a lower melting point than the neighbouring compositions.

In a binary alloy system two different solid phases are formed during cooling. In this case a liquid of fixed composition (called eutectic composition) freezes at a particular temperature (called eutectic temperature) to give two solids of definite composition. In a given alloy system more than one eutectic composition may occur.

Zone refining may be defined as ultra purification of high purity materials. It makes use of segregation phenomena. The technique is conducted by using a localised heating source, such as an induction coil, radiant heater, or electron beam to produce a molten zone somewhere along the length of the bar of the material, which is to be purified. The zone is slowly swept along the length of the bar, and the process may be repeated as often as required.

The material can be supported horizontally in a refractory mold or when extreme purity is required it may be held vertically

in vacuum or in an innert atmosphere. The molten zone is caused to traverse along the length of the solid bar by moving the source of heat at a given rate along the bar in forward direction, while back motion is very fast, so all the impurities which lower the melting point of the material gets segregated in the last part to be solidified. In zone levelling the molten zone is moved in both direction with the same speed, which levels the impurity content of the bar.

REVIEW

2.1 Eutectic Solidification:

Formation of Lamellar:

The first theory of lamellar eutectic solidification appears
to have been given by Tammann[1], who proposed that the two phases
crystallise alternately. Vogel[1] expressed a different opinion of
the growth mechanism, as he considered that the eutectic alloy
of Cd-Zn solidified by the simultaneous crystallisation of both
phases. During solidification the α phase rejects atoms of B and
β phase rejects atoms of A. Under steady state growth conditions,
the rate of rejection of B atoms by α phase is equal to the rate
of rejection of A atoms by the β phase.

Imagine a membrane to be placed in liquid colinear with
the α-β phase boundary, so that no lateral diffusion of solute
can occur. In this case the solute distribution in the liquid ahead
of α and β lamellae will increase to their steady state value
given by,[3]

$$C_L^\alpha = C_0 \left| \frac{1-K_\alpha}{K_\alpha} \right| \exp\left(- \frac{RX}{D}\right) + C_0 \qquad (1)$$

$$C_L^\beta = C_0 \left| \frac{1-K_\beta}{K_\beta} \right| \exp\left(- \frac{RX}{D}\right) + C_0 \qquad (2)$$

where C_L^α = Concentration of B ahead of α phase

C_L^β = Concentration of A ahead of β phase

X = Distance from solid liquid interface

K_α = Partition coefficient of B in α

K_β = Partition coefficient of A in β

D = Liquid diffusion coefficient,

R = Rate of advance of the interface,

C_e = Eutectic concentration.

The solute distributions are represented in Figure 1, i.e. a build-up of β constituent ahead of α phase and deficiency ahead of β phase. But in actual case there will be lateral diffusion between the two regions rich in solute and because of lateral diffusion the solute concentration has its highest value at the centres of the lamellar and the composition at the interface boundary must be equal to C_e, the eutectic concentration, because it is in contact with both α and β phases simultaneously. The concentration across the solid-liquid interface will be as shown in Figure 2.

In general the widths of the individual lamellar of two different phases will not be equal, nor will the concentration profiles of solute elements ahead of the two phases be equal.

Lamellar to Rod Transition:

In some cases the eutectic freezes with a rod-like morphology instead of a lamellar morphology at all values of growth rates, and in other cases lamellar break down into rods at certain growth rates.

Considering the same volume fraction of α and β phases for both morphologies, it is immediately apparent that the ratio of the phase particle width $\lambda_\alpha/\lambda_\beta$ changes when the eutectic assumes the rod form rather than the lamellar form. The average undercooling due to diffusion for the rod form may therefore be compared with that for the lamellar form,
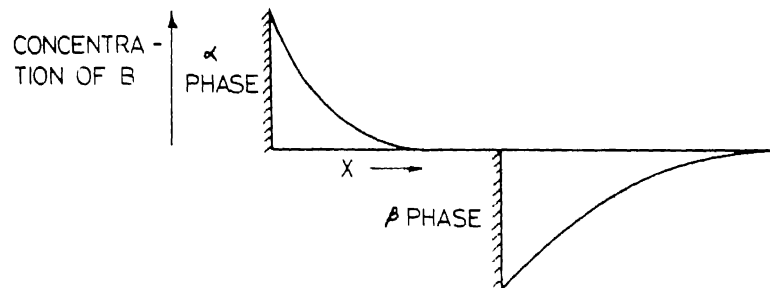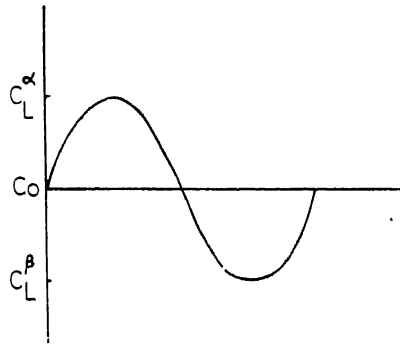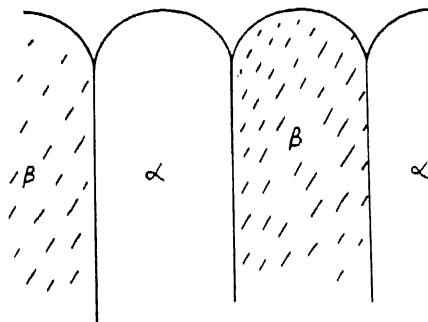
CONCENTRA - TION OF B

α PHASE

X ⟶

β PHASE

FIG 1 _ DISTRIBUTION OF B CONSTITUENT AHEAD OF α & β PHASES[3]

FIG 2 _ (a) CONCENTRATION DISTRIBUTION AHEAD OF EUTECTIC INTERFACE[1]

(b) SHAPE OF EUTECTIC INTERFACE[1]

$$\Delta T_{D(rods)} \simeq \left(\frac{\theta'\gamma'}{\theta\gamma}\right) \Delta T_{D(lamellar)} \qquad (3)$$

where
γ = Shape factor for lamellar morphology,

γ' = Shape factor for rod morphology,

θ = Constant factor for lamellar morphology,

θ' = Constant factor for rod morphology,

ΔT_D = Average undercooling of the interface required to drive the diffusion during steady state growth.

The shape parameter γ has changed since the ratio $\lambda_\alpha/\lambda_\beta$ and therefore the ratio of lead distance of two phase ahead of the interface, (d_α/d_β) has changed. The ratio d_α/d_β has decreased, thus $\gamma'/\gamma < 1$, so $\Delta T_{D(rod)} < \Delta T_{D(lamellar)}$ i.e., the diffusion between the phases is easier for rod morphology than the lamellar morphology.

The relationship between the undercooling due to boundary formation may also be determined. The number of rods intersecting unit area of interface is $4/\pi\lambda^2$, thus the length of $\alpha\beta$ phase boundary per unit area solid liquid interface is $4\lambda_\beta/\lambda^2$. Since the departure of the $\alpha\beta$ phase boundary from its preferred orientation will produce an increase in average interfacial energy per unit area to $\bar{\sigma}_{\alpha\beta}$, the $\alpha\beta$ interfacial energy per unit volume of solid is $\frac{\sigma_{\alpha\beta}}{\lambda}(1 + \theta_\beta^\alpha)^{1/2}$. Thus the relative undercoolings due to the formation of $\alpha\beta$ phase boundary for the two forms of identical λ

$$\Delta T_{B(rod)} = \left[\frac{2\bar{\sigma}_{\alpha\beta}}{\sigma_{\alpha\beta}}(1 + \theta_\beta^\alpha)^{1/2}\right] \Delta T_{B(lamellar)} \qquad (4)$$

where
$\sigma_{\alpha\beta}$ = Interfacial energy per unit area,

$\bar{\sigma}_{\alpha\beta}$ = Increased average interfacial energy per unit area produced due to the departure of the $\alpha\beta$ phase boundary from its preferred orientation,

θ_β^α = Ratio of volume fraction of two phases,

If the shape factor γ is once again considered as constant, it is readily apparent that,[3]

$$\delta T_{m(rods)} \simeq \left[\frac{2\theta'\gamma'\overline{\sigma}_{\alpha\beta}}{\theta\gamma\overline{\sigma}_{\alpha\beta}} (1 + \theta_\beta^\alpha)^{1/2} \right] \delta T_{m(lamellar)} \quad (5)$$

From equation 5, if the bracketed expression is less than unity, the rod form will produce steady state growth at higher transformation temperature than the lamellar form and will thus be more stable than the lamellar form. For the eutectics having a large value of θ_β^α, the rod morphology will be favoured.

Now to see why a eutectic will assume the lamellar form at low rates of growth and transforms to the rod morphology at higher rates of growth, one need a knowledge of the functional form of γ. Such a transition would only be possible if $\frac{\theta'\gamma'}{\theta\gamma}$ is a function of λ or R. This might allow $\delta T_{m(lamellar)} < \delta T_{m(rods)}$ at low rates and $\delta T_{m(rods)} < \delta T_{m(lamellar)}$ at high rates.[3]

Rods to Globular Transition:

As the rate of freezing continues to increase, the separation distance of the rods will decrease[3], and the undercooling of the solid-liquid interface will increase. As the interface temperature decreases, the α interface will become supercooled with respect to β phase and vice-versa. As the rods become narrower, the probability of nucleating the β phase on the α matrix will increase[3]. Thus at high rates of growth, the repeated nucleation will lead to the formation of globular of the discontinuous phase dispersed in the matrix of the continuous phase.

In the system where the $\alpha\beta$ phase boundary energy is quite large, a steady state lamellar interface cannot exist. In this case, the discontinuous phase particles may nucleate on the continuous phase substrate, but continued growthwill not lead to a stable morphology. Instead repeated nucleation of the discontinuous phase particles must occur at all rates of growth producing a globular structure. The globular morphology will therefore be favoured by small value of $\sigma_{iL}(i = \alpha, \beta)$ and large value of $\sigma_{\alpha\beta}$.[3]

Anomalous Eutectic:

In many systems, one of the phases appears to be randomly distributed in the two-dimensional microsection. If the nucleation plays a major role in such a random array, one can argue that when the primary phase is unable to serve as a nucleating agent for the secondary phase and the second phase is nucleated hetrogeneously in the liquid, this results in a random orientation of the discontinuous phase particles.[3] Such eutectic has been termed as 'anomalous eutectic'. For nucleation to occur in the liquid rather than on the primary substrate, it is required that the α-β interfacial energy, $\sigma_{\alpha\beta}$, be large compared to the β-crystal interfacial energy $\sigma_{\alpha\beta}$.

Divorced Eutectic:

The divorced (degenerate) eutectic shows no coupling[4], in fact the two phases attempt to minimise their area of contact and to form separate crystals. It has been suggested that slow cooling favour this type of structure. This structure results when the two phases freeze one at a time and solidification of one is completed before the second starts. The formation of divorced

eutectic is not a characteristic of any system, nor is it directly related to the properties of the components or to the location of the eutectic point. Divorced eutectics predominate when the phase that nucleates the eutectic requires higher undercooling for its nucleation, and when the alloy composition is far from the eutectic on the side of the non-nucleating phase.

2.2 Classification of Eutectic Alloys:

Scheil's Classification:

Scheil[5] has devided all binary eutectic structures into 'normal' and 'anomalous' based on the concept of a coupled region of eutectic crystallisation.

A normal eutectic structure is typically lamellar in form, the two eutectic phases are arranged in alternate parallel sheets or lamellae, a structure comparable to that of eutectoid pearlite in steels. A frequent variation is the rodlike structure, in which one phase crystallises as a series of parallel rods embedded in a continuous matrix of the other phase. Such structure is normally found in impure alloys[6]. This structure is also observed in the alloys where the volume fraction of the second phase is low[7]. The essential feature of a normal structure is that the two eutectic phases presumably crystallize simultaneously by the advance of a common interface into the melt.

An anomalous eutectic structure according to Scheil is typified by the absence of any such common interface, the second phase particles are irregularly distributed in the parent matrix.

Reference was also made to a third class of structure which Scheil called 'degenerate', but this class was very poorly defined

Scheil referred repeatedly to a 'globular' type of normal eutectic structure, which was conceived as a uniform distribution of discrete globular of one phase in a continuous matrix of the other. However, globular structure are very rarely found, for example, Fe-C and $Cu-Cu_2O$ eutectics.

Nucleation Criteria:

The structure of eutectic alloys is somewhat dependent on nucleation of the phases[8]. Normal eutectic forms when one phase acts as nucleating agent for the other one and the two phases grow more or less together with a definite orientation relationship between them anomalous eutectic forms when both phases are nucleated by foreign impurities and there is no orientation relationship between the phases. Degenerate eutectics result when the second phase is not nucleated until solidification of the first phase is completed.

In any eutectic system two or even all three type of eutectic structures can form, because the appearance of the one or the other type is partly nucleation controlled. The structure depends mainly on the type and amount of impurities present, but is not closely related to the characteristic of the components or of the equilibrium diagram. Hence the addition or removal of impurities can upset the nucleation and shift the alloy structure from one type to another.

The results of the research on nucleation[9] showed that nuclea tion is strictly a one way street, if α nucleates the β phase, β phase has no nucleating effect on α. Thus unilateral nucleation was shown by the fact that, whereas the presence of primary crystals of

significantly reduced the undercooling necessary for freezing of β, the presence of β crystal did not reduce and occasionally even increased the supercooling for the freezing of α. If the freezing of the eutectic (nucleation of β) took place with an appreciably small undercooling when primary α crystals were present, the nucleation of β was attributed to α primary particle[10]. If no difference in undercooling was measured with or without primary crystals, nucleation of β in the eutectic was attributed to foreign impurities in the melt. The nucleation data are reported in Table 1.

As the melt of eutectic concentration is supercooled, the nuclei of one phase will form in the liquid. As the crystals of this phase begin to grow, solute distribution will be built up ahead of them making the interface more greatly supercooled with respect to the second phase. The initial nuclei will grow as rods or platelets as illustrated in Figure 3(a), since these are the shapes that will grow with the least solute build up at the growing edge, and thus the least undercooling.

If the primary phase serves as an effective nucleus for the second phase, the second phase will nucleate on the surface of the primary phase and absorb the supercooling. Figure 3(b) illustrates the nucleation of the second phase on the face of the primary phase and the edge wise growth of this nucleus to absorb the supercooling.

There are now two plates growing both edgewise and sidewise. The formation of new layers of alternate phase may readily occur by overlap of one phase at the edge of the other phase as illustra

Table 1

Undercooling for Nucleation[10]

Alloy	Primary phase	Undercooling for nucleation °C below eutectic temp.
Zn - Bi	Zn	$\geq$ 63
	Bi	0.25
Sn - Bi	Sn	$\geq$ 17
	Bi	6.0
Sn - Zn	Sn	$\geq$ 5
	Zn	3.5
Pb - Sb	Pb	$\geq$ 21
	Sb	6.0
Bi - Pb	Pb_2Bi	4.5
	Pb	$\geq$ 30

(a)   PRIMARY PHASE
      PARTICLE

(b) NUCLEATION OF
     SECONDARY PHASE

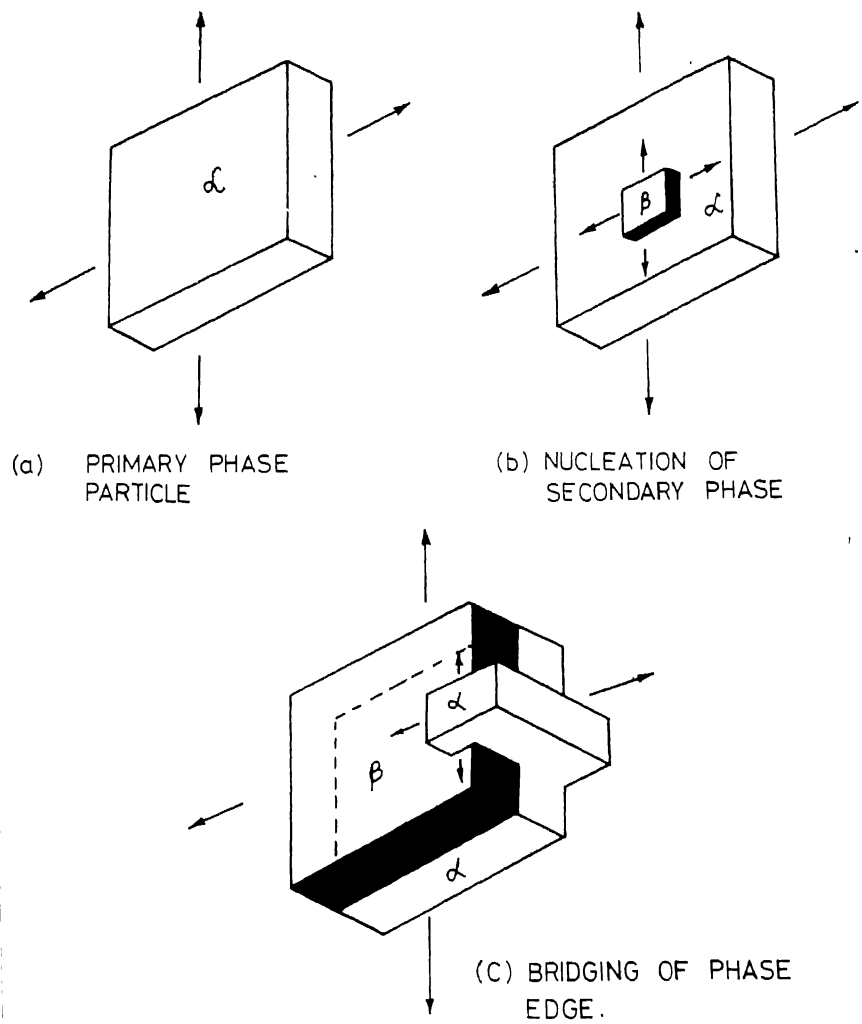(C) BRIDGING OF PHASE
     EDGE.

FIG. 3 _ PROPOSED MECHANISM OF ALTERNATE
         LAYER FORMATION[3]

in Figure 3(c). Thus a multilayered unit may be built by this overlapping mechanism. Such a growth unit would produce lamellar of the discontinuous phase having a fixed orientation in a grain[3].

X-ray studies, of a number of lamellar eutectic systems, have determined the crystallographic relationship that exists between the lattices of the two lamellar. Their determination of the corresponding planes and directions in the two lattices have been tabulated in Table 2.

Nucleation effect can be summarised as below[11]

	Orientation Relationship between phases	No orientation relationship between phases
One phase acts as nucleus	Normal	Anomalous
No phase acts as nucleus	-	Degenerate

The empty space shows that no orientation relationship can exist between the phases without a simultaneous nucleation effect.

It is, however, doubtful if nucleation really plays a great part in determining the micro-morphology of the phases except during initial stages of growth of the eutectic grain[21]. This aspect will be discussed later.

Chadwick's Classification:[1]

Chadwick[1] has proposed the division of eutectic structure into 'continuous' and 'discontinuous' type, but this classification leads to essentially the same classification as that of Scheil. Not only that, but many seemingly discontinuous structure such as Al-Si have in fact been found to be continuous[38].

Table 2

Orientation Relationship in Eutectic of Binary Alloys.[3]

System	Phases Formed	Relations
Ag - Cu	Two f.c.c.	All planes and directions parallel.
Al - Cu	Al (f.c.c) θ (b.c. tetragonal)	(001) Al || (001) θ [100] Al || [100] θ
Ag - Al	Al (f.c.c) $\gamma_{(AgAl)}$ (c.p.h.)	(111) Al || (0001) γ [110] Al || [1120] γ
Cd - Zn	Two c.p.h.	(0001) Cd || (0001) Zn [0110] Cd || [0110] Zn
Bi - Cd	Bi (rhombohedral) Cd (c.p.h.)	(1010) Bi || (0001) Cd [0001] Bi || [0110] Cd
Cd - Sn	Cd (c.p.h.) Sn (b.c.t)	(100) Sn || (0001) Cd [001] Sn || [0110] Cd
Sn - Zn	Sn (b.c.t) Zn (c.p.h.)	(100) Sn || (0001) Zn [001] Sn || [0110] Zn

Lead Distance:

Davies[11] has classified the eutectic structure on the
basis of lead distance. The growing lamellar do not always move in
a linear front, very often one phase will precede the other (See
Figure 4). Hence longitudinal diffusion along the leading phase
will exist in addition to the lateral proceeding in front of the
solid-liquid interface.

Tiller[3] has derived an equation for the lead of one phase
over the other, but it cannot be solved explicitly with regards to
the metal lead. Tiller assumed that the tips of the lamellar were
convex, with relatively deep grooves between neighbouring lamellar
Figure 4(a). However, the direct observation of the solidification
front shews that at least some systems exhibit a rather sharp edge
lamellar Figure 4(b). Hence the longitudinal diffusion distance
is equal to the lead distance d_α. If eutectic concentration is
assumed to be where the two phases meet, the total diffusion dis-
tance is given by,

$$I_\alpha = \frac{\lambda_\alpha}{2} + d_\alpha, \quad I_\beta = \frac{\lambda_\beta}{2} \tag{6}$$

Following Tiller's reasoning that the flux of solute into
and out of the corner where the lamellar meet are equal, the concen-
tration difference between the mid point of the lamellar and corner
is $\Delta c_L^i = c_L^i - C_E$ where c_L^i is the concentration of B constituent
in front of i phase and C_E is the eutectic concentration. With
indexes corresponding to the two phases the concentration gradient
is given by,

$$\frac{\Delta c_L^\alpha}{I_\alpha} = -\frac{\Delta c_L^\beta}{I_\beta} \tag{7}$$
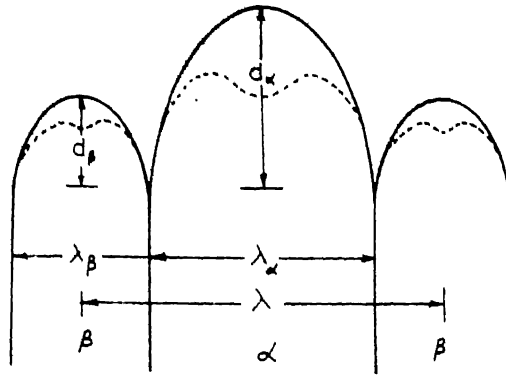
(a) MOST PROBABLE INTERFACE SHAPE DURING STEADY STATE GROWTH OF A LAMELLAR EUTECTIC[3]
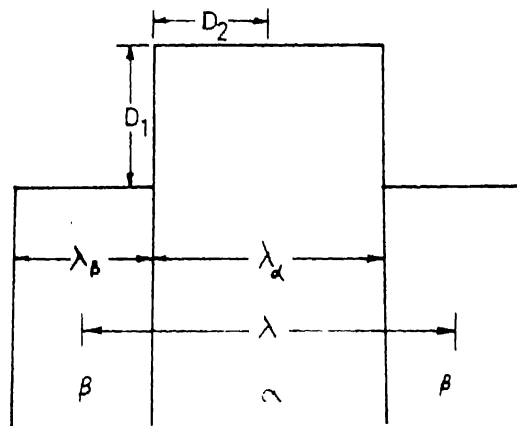
(b) INTERFACE SHAPE[11]

FIG 4

From equation 6,

$$\frac{I_\alpha}{I_\beta} = \frac{\lambda_\alpha + 2d_\alpha}{\lambda_\beta} \qquad (8)$$

From equations 7 and 8,

$$\frac{\Delta C_L^\alpha}{\Delta C_L^\beta} = - \frac{\lambda_\alpha + 2d_\alpha}{\lambda_\beta} \qquad (9)$$

The slope of the liquidus in the phase diagram may be related to ΔC_L^α and T_m as shown in Figure 5. Where T_m is the degree of supercooling. A definite amount of supercooling is always required to drive the growth process but this amount may be small. From Figure 5,

$$m_\alpha = \frac{\Delta T_m}{\Delta C_L^\alpha} \quad ,$$

$$m_\beta = \frac{\Delta T_m}{\Delta C_L^\beta} \quad ,$$

eliminating ΔT_m,

$$\frac{\Delta C_L^\alpha}{\Delta C_L^\beta} = \frac{m_\beta}{m_\alpha} \quad , \qquad (10)$$

and combining equations 9 and 10,

$$\frac{m_\beta}{m_\alpha} = - \frac{\lambda_\alpha + 2d_\alpha}{\lambda_\beta} \qquad (11)$$

The ratio of the lamellar thickness is equal to the volume fraction i.e.,

$$\frac{\lambda_\alpha}{\lambda_\beta} = \frac{V_\alpha}{V_\beta} \qquad (12)$$
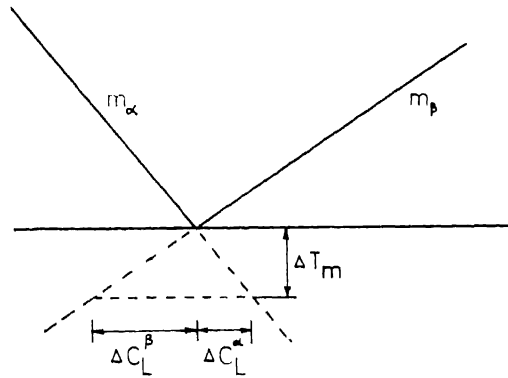
FIGURE_5_ LIQUID SLOPE RELATED TO ΔT_m
& $\Delta C_L^{i\,(11)}$

combining equations 11 and 12,

$$d_\alpha = -\frac{\lambda_\alpha}{2} \left| \frac{m_\beta V_\beta}{m_\alpha V_\alpha} + 1 \right| \tag{13}$$

This expression based on very simple assumption, gives the lead of the α phase over the β phase during lamellar growth. The magnitude of lead is determined by the parameter $m_\beta V_\beta/m_\alpha V_\alpha$, which may be calculated by means of values derived from the phase diagram. It has been shown, taking a number of eutectic systems into consideration, that most systems with value of the parameter $m_\beta V_\beta/m_\alpha V_\alpha < 4$ i.e. $d_\alpha < 1.5 \lambda_\alpha$ are normal eutectics and all systems with values of the parameter > 4 i.e., $d_\alpha > 1.5 \lambda_\alpha$ are anomalous or degenerate.

Recalculation[12] of the lead distance, regarding the minor phase as the leading phase in all cases, resulted in negative value in some cases. The range of normal eutectic extend from $d_\alpha/\lambda_\alpha = 1.5$ to $d_\alpha/\lambda_\alpha = -0.25$, the systems with parameter outside this range are apparently anomalous or degenerate. However, some exceptions to this criteria have been frequently found as will be illustrated later (See Table 3).

Entropy of Fusion:

The classification[13] is based on the entropy of fusion of the two eutectic phases. There are three groups of eutectics, those in which both phases have low entropy of fusion, those in which one phase has high and the other phase has low entropy of fusion, and those in which both phases have high entropies of fusion.

Lamellar or rodlike structures (regular structure) are formed in which both phases have low entropies of fusion. Irregular or

Table 3

Classification of Eutectics

S. No.	System	Diagram	Leading phase	Devies criteria			Type (predicted)
				$\frac{\lambda_\alpha}{\lambda_\beta} = \frac{V_\alpha}{V_\beta}$	$\frac{m_\beta}{m_\alpha}$	$\frac{d_\alpha}{\lambda_\alpha}$	
1	2	3	4	5	6	7	8
I	Pb–Sb	Simple	Sb	0.143	–.72	2.0	Irregular
II	Bi–Cd	Simple	Bi	1.33	2.29	0.57	Regular
III	Zn–Zn$_3$Sb$_2$	Complex	Zn$_3$Sb$_2$	0.051	–0.213	1.6	Irregular
IV	Bi–BiPb$_2$	Complex	Bi	0.363	–0.72	0.5	Regular
V	Bi–Sn	Simple	Bi	0.667	–1.04	0.28	Regular
VI	Bi–Zn	Simple	Zn	0.038	–0.11	0.95	Regular
VII	Sn–Zn	Simple	Zn	0.101	–0.378	1.4	Regular

S. No.	Structure (Observed)	Eutectic Temp. °K	Eutectic comp. wt.%	Hunt and Jackson's criteria		Type	Structure (predicted)
				Entropy of melting			
				1st phase	2nd phase		
	9	10	11	12	13	14	15
I	Non uniform	525	11.1% Sb	Pb 1.9	Sb=5.25	NF–F	Irregular
II	Imperfect lamellar	417	40% Cd	Bi=4.78	Cd=2.40	F–NF	Irregular
III	Flakey	686	2.6% Sb	Zn=2.55	Zn$_3$Sb$_2$=3.63	NF–NF	Regular
IV	Complex regular	398	43.5% Pb	Bi=4.78	Pb$_2$Bi=4.12	F– F	Irregular
V	Complex regular	412	43.0% Sn	Bi=4.78	Sn=3.41	F–NF	Irregular
VI	Broken lamellar	527.5	2.7% Zn	Bi=4.78	Zn=2.55	F–NF	Irregular
VII	Broken lamellar	471	9% Zn	Sn=3.41	Zn=2.55	NF–NF	Regular

complex regular structures are formed in alleys in which one phase
has high entropy of fusion and the other has low entropy of fusion.
In the third group of eutectics in which both phases have high
entropies of fusion, each phase grows with a faceted solid-liquid
interface. Structures of some eutectics on the basis of above cri-
terias are tabulated in table 3.

Pilonenko[14] has classified the structure on the basis of
entropy ratio. If S_α/S_β = 1-1.5 (S_α and S_β are fusion entropies
of eutectic constituents), regular structures are formed irrespec-
tive of fusion entropy level. If $S_\alpha/S_\beta \geq 1.5$, eutectic structures
with phases of irregular orientations are obtained.

Free Energy Criteria:

The reason for the failure of Hunt and Jackson's classifica-
tion[13] seems to be the consideration of entropies of fusion of the
pure components. In some materials the solubility in the eutectic
phases is quite large, and since the eutectic temperature can be
considerably below the melting point of pure material, the use of
entropy of fusion for pure component rather than for the solid solution
at the eutectic temperature appears to be questionable.

Jackson[13] has differentiated between the two types of the
solid-liquid interface by the shape of the relative free energy
curves. If the energy minimum occurred at position corresponding
to half the surface sites filled, then an atomically rough solid
liquid interface would exist, where as minima occurring at positions
corresponding to the surface being almost empty implies a smooth
or faceted interface.

Kerr and Winegard[15] have classified the eutectic alloys on the basis of free energy of the two components. Using Jackson's criteria, Bi is close to the border line between rough and faceted interface, its minima is poorly defined but it centres around the position corresponding to half the surface sites filled, leading to the result that Bi-Sn, Bi-Pb will form regular structure, while these structures are complex regular or irregular. Also the minima of the energy for Ag phase in Bi-Ag also occurs at position corresponding to 0.2 and 0.8 of the surface sites filled, implying that the Ag phase might grow with a faceted solid liquid interface, leading to the complex regular structure in case of Bi-Ag eutectic alloy, while in this case the structure is regular.

Kerr and Winegard[15] have plotted the relative free energy v/s fraction of surface sites occupied for Bi-Ag and Bi-Sn alloys as shown in Figure 6, and concluded that the eutectic will be regular if the interfaces have approximately the same relative free energies and that the eutectic will be more irregular if the calculated relative free energies are very different.

Distribution Coefficient:

Bell and Winegard[16,17] examined the possibility of separating the eutectics into structural groups in terms of distribution coefficient K, and growth undercooling phenomena of the two phases. They observed that for a number of systems the phase of that element, the K_0 value of which in the other phase is smaller, is the leading phase and by plotting $(1-K_0)/K_0$ against $G/R^{1/2}$ (i.e., factors controlling undercooling phenomena at the interface) they showed that grouping of typical eutectic structure is possible, although of limited accuracy.
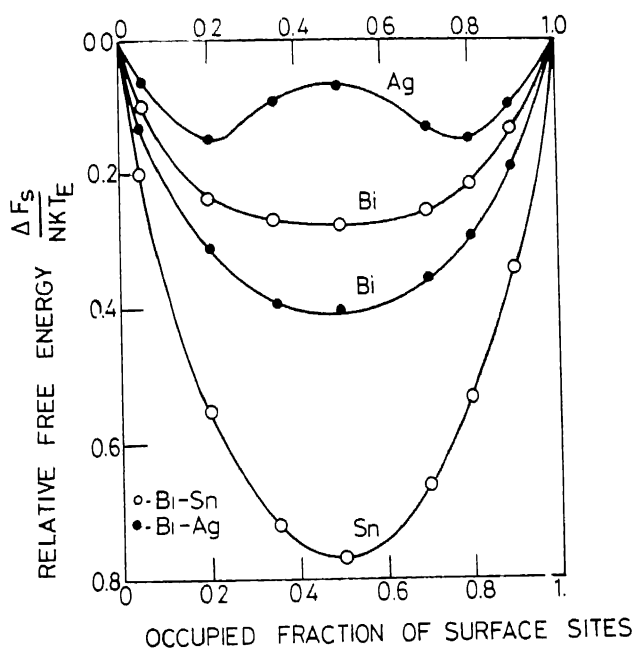
FIG 6 _ RELATIVE FREE ENERGY VERSUS
FRACTION OF SURFACE SITES OCCUPIED[15]

Activity Coefficient:

A correlation is observed between activity coefficients for the liquid eutectic alloy and the type of structure that is obtained. In Table 4 the type of microstructure exhibited by several eutectic systems are compared with the activity coefficients of their components in the liquid phase referred to the pure liquid metal.

It is evident from Table 4 that eutectics which solidify with a regular lamellar structure are associated with liquid phase which exhibit positive deviation from ideality, whilst irregular eutectics are associated with liquid phases which exhibit zero or negative deviation from ideality. Since the activity measurements were made at temperatures above the eutectic temperature, the behaviour of these liquids at lower temperature will show larger deviations from ideality than is suggested by the data in Table 4, making the correlation even more marked.

A large interface undercooling is associated with the formation of non uniform structure. The undercooling (T_D), due to the accumulation of solute in the liquid ahead of each lamella, is inversely proportional to D, the diffusion coefficient for the liquid alloy. It has been predicted[19], however, that for liquid alloys a solute with a large positive partial molar heat of solution (i.e. a positive deviation from ideality) will diffuse faster than one with a negative or zero partial molal heat of solution. This relation between activity and diffusion rate has been experimentally confirmed for dilute solute concentration in tin solvent[20]. Thus the correlation observed in Table 4 may be due to a variation in the diffusion rate in the liquid for the different systems.

Table 4[18]

Relationship between activity coefficient data for binary liquid
Eutectics, and eutectic structural types

System A – B	T_E °K	A at T°K	B at T°K	T°K	Eutectic Structure
Bi – Zn	527	1.005	2.655	873	Regular
Cd – Pb	521	1.979	1.093	773	Regular
Cd – Sn	450	1.302	1.060	773	Regular
Cd – Zn	539	1.110	2.001	800	Regular
Pb – Ag	577	1.010	3.160	1000	Regular
Pb – Sn	456	1.070	1.660	723	Regular
Sn – Zn	471	1.011	2.004	700	Regular
Bi – Au	514	0.981	0.921	973	Irregular
Bi – Cd	417	0.958	0.928	773	Irregular
Bi – Sn	412	1.058	1.056	608	Irregular
Bi – Pb	398	0.857	0.754	700	Irregular
Al – Si	850	0.989	0.350	1800	Irregular
Pb – Sb	524	0.994	0.823	900	Irregular

Growth Phenomena:[21,22]

If the entropy of fusion value of two phases differ widely, their internucleation and growth characteristic also differed, and it appeared, therefore, desirable to evaluate entropy value for all eutectics, the structure of which are known. The entropy factor ε and ε' defined,

$$\varepsilon = \frac{\Delta S_\beta}{\Delta S_\alpha} \quad \text{and} \quad \varepsilon' = \frac{(L_\beta/T_e)}{(L_\alpha/T_e)} = L_\beta/L_\alpha \qquad (14)$$

were evaluated for 151 eutectics. The values of ε and ε' are compared in Figure 7. The entropy of fusion value of solid solution was calculated from the pure metal data, and that of intermetallic compound included an extra term,

$$- 4.573 \, (N_1 \, \log N_1 + N_2 \, \log N_2) \qquad (15)$$

where N_1 and N_2 are the atomic fractions of the components. In the case of ε' the eutectic, instead of the component melting, temperature was used for entropy calculation. Of the two factors, ε' appears to be more successful in separating eutectic into structural groups. About 90 percent of normal eutectics examined occur for value $\varepsilon' < 1.4$ and 65 percent of anomalous eutectics for $\varepsilon' > 1.4$.

The results shown in Figure 7 suggests that phases of similar rather than dissimilar properties could be expected to give normal eutectics, and this hypothesis was tested by evaluating, the conditions for internucleation of eutectic phase. The relation between the interfacial energies for nucleation of β on α can be expressed by the equation,

$$\cos \theta_\beta = \frac{\sigma_{\alpha L} - \sigma_{\alpha \beta}}{\sigma_{\beta L}} = 1 \qquad (16)$$
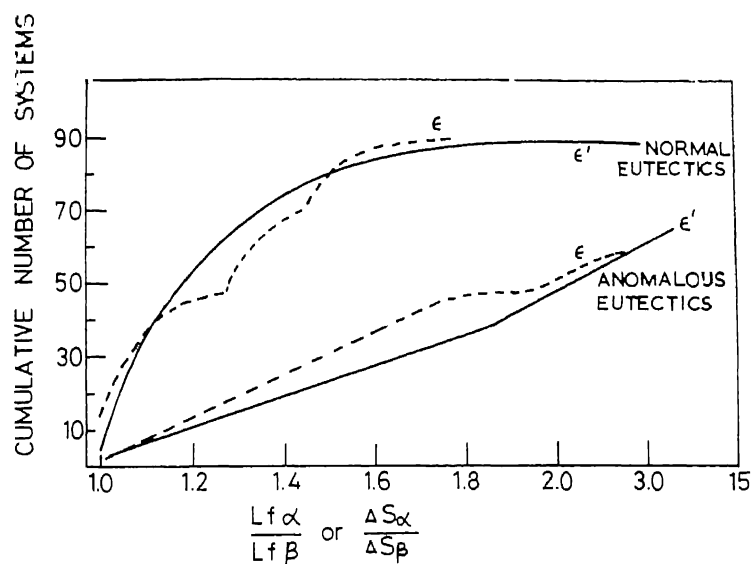
FIG.7. CLASSIFICATION OF EUTECTICS IN TERMS OF ENTROPY FACTOR[21]

Similarly for nucleation of α by β,

$$\cos \theta_\beta = \frac{\sigma_{\beta L} - \sigma_{\alpha\beta}}{\sigma_{\alpha L}} = 1 \qquad (17)$$

No mutual nucleation condition can be stated as,

$$\frac{\sigma_{\alpha L} - \sigma_{\alpha\beta}}{\sigma_{\beta L}} + \frac{\sigma_{\beta L} - \sigma_{\alpha\beta}}{\sigma_{\alpha L}} < 2 \qquad (18)$$

or rearranged into,

$$\frac{(\sigma_{\alpha L} - \sigma_{\beta L})^2}{\sigma_{\alpha L} + \sigma_{\beta L}} < \sigma_{\alpha\beta} \qquad (19)$$

Approximate value for interfacial energies can be obtained from latent heat of fusion (L), and gram atomic volumes (V), and using the following relations:

$$\sigma_{\alpha L} = 0.179 \, \phi_\alpha \qquad (20)$$

and

$$\sigma_{\alpha\beta} = 0.268 \, (\phi_\alpha - \phi_\beta) \qquad (21)$$

where,

$$\phi = L/V^{2/3} \qquad (22)$$

The condition for no nucleation becomes after substitution:

$$\psi = \frac{|\phi_\alpha - \phi_\beta|}{\phi_\alpha + \phi_\beta} < 1.22 \qquad (23)$$

Factor ψ, plotted in Figure 8 appears to give a clearer separation of normal and anomalous eutectics, than the factor C'.

The physical significance of this result is that normal eutectic fall into the range of 'non-mutual nucleation' i.e., neither phase need to nucleate the other. Hence observed orientation relationship for normal eutectics result not from nucleation restrictions
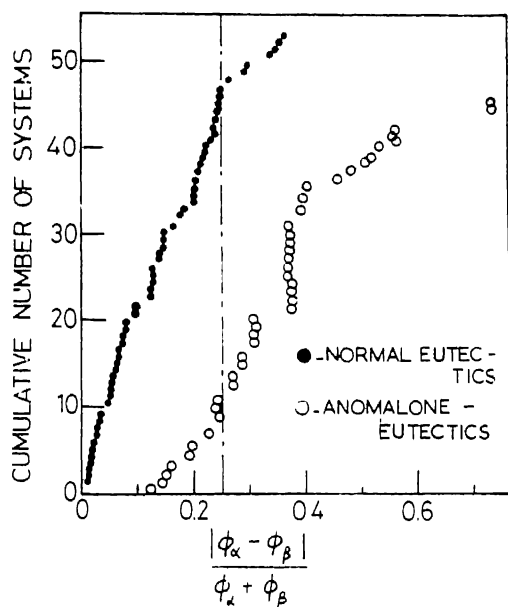
FIG. 8 _ CLASSIFICATION OF EUTECTICS IN TERMS
OF INTERFACIAL ENERGY [21]

but from growth restrictions. A view confirmed by the multiplicity of orientation relationships during the first few centimeters of growth[21]. The nucleation phenomenon can affect undercooling behaviour and other features in the cast structure (grain size and shapes). But in general it is difficult to see how nucleation phenomenon could be used as a basis for explaining or predicting the type of eutectic structure. The growth phenomena on the other hand influence the mutual arrangement of two phases.

2.3 Parameters Determining Eutectic Structure:

Different parameters which affect the eutectic structure are,

(a) Impurity Contents,

(b) Growth Rate,

(c) Temperature Gradient, and

(d) Energy of Twin Formation.

(a) Impurity Contents:

Impurities have significant effect on the structure of eutectic alloys. During solidification, the solidifying phase rejects the impurities to the remaining liquid. These impurities segregate and collect in front of solid liquid interface. This segregation of impurities will cause constitutional supercooling and because of this supercooling the planar solid-liquid interface will no longer be stable, and will change to stable cellular interface, resulting in cellular structure[18,23].

As shown by Chadwick[1] if the impurities have different segregation coefficient in the two phases, the impurities build-up ahead of two phases will be different, which will give rise to different

constitutional supercooling. So one phase must lead the other, and for a stable solid-liquid interface the lagging phase must be in the form of rods or fibres. Hence this type of impurities will change a lamellar structure into rodlike structure as has been verified by different workers on different systems.[24,25,26]

(b) Growth Rate:

The structure of an eutectic alloy depends upon the growth rate. The alloy which solidifies with a regular structure at slow growth rate changes to irregular or complex regular as the growth rate increases.[27,28] As the growth rate increases the planar solid-liquid interface breaks down and alloy solidifies with the cellular interface.[29,30] As in high growth rate impurities do not have sufficient time to diffuse away from the interface into the liquid, they go on accumulating at the interface. This accumulation of impurities cause constitutional supercooling and the planar interface becomes unstable and the alloy solidifies with cellular structure.[31] The growth rate also changes the structure from lamellar to rodlike structure.[32,33,34] It has been shown[35] that in case of Sn-Zn eutectic alloy, the broken lamellar morphology will become more rodlike at the higher growth rates and less broken at the lower growth rate. As shown by Cooksey et.al.,[7] the lamellar eutectic exhibits a gradual modification or degeneration at very slow freezing rate. The breakdown of lamellar arrangement begins at freezing rates below 5 mm/hr. However such break down occurs at lower and lower speeds as purer alloys are frozen.

(c) Temperature Gradient:

The structure also depends upon temperature gradient, Fig.9 which has direct effect on constitutional supercooling.[27,36] The
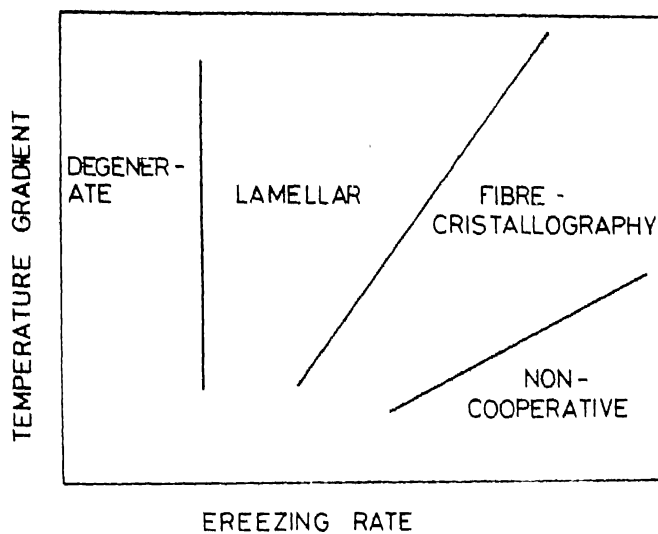
FIG 9 _ DIFFERENT MICRO – STRUCTURE WITH
VARYING FREEZING RATES AND TEMPERATURE
GRADIENT [27]

sharp temperature gradient reduces the constitutional supercooling. An alley which normally freezes with cellular structure[37] by applying a sharp temperature gradient and vice-versa. It has been shown[27] that the lamellar arrangement can be modified to a fibrous structure with decrease of temperature gradient. In the case of Al-Si eutectic alley, at a given freezing rate the width of the plate is found to vary inversely with the imposed temperature gradient, the silicon might not lead the aluminum enough to develope well defined plates and possibly might then occur as fibres.[27]

(d) Energy of Twin Formation:

In an alley where the energy of twin formation is quite low, the twin formation takes place very easily and at smaller undercooling, which will result in irregular or complex regular structure.[38] On the other hand, if energy of twin formation is quite high, no branching or less branching takes place, resulting in regular structure.

In the case of Al-Si eutectic[38], the silicon phase is able to change its growth direction during growth by means of multiple twinning and so local overgrowth diverts the non-metal but does not terminate its growth. This ability to change direction during growth to produce an interconnected irregular eutectic is found in many metal-non metal eutectics such as Ag-Si, Au-Si, Al-Ge and Fe-Graphite, and could well be occurring in the majority of this class of eutectic systems.

As seen earlier, a variety of structures can be formed by changing the solidification conditions. The range over which different regions apply varies widely from system to system. It is very rarely possible to illustrate more than one transition in growth mechanism with a given alloy, because the necessary range of conditions are beyond those which can easily be obtained experimentally.

2.4 Freezing of Irregular Structure Eutectic Alloys:

The eutectic alloys which form irregular structure generally freeze with non-planar solid-liquid interface, the irregular eutectic results from the non-coupled growth of the two phases in which one phase leads much ahead of the second phase, making the solid-liquid interface non-planar. This type of structure is found in eutectic systems having faceted and nonfaceted components or phases.[39]

Facets form when there is an energy barrier for the addition of a new solid layer on an existing solid. When a barrier is present, growth proceeds by the lateral movement of steps across a crystallographic plane.

Hulme and Mullins[40] have shown that faceting in single phase material can only occur when both interface curvature are convex with respect to the solid. Facets do not occur when the interface is concave, because the adjacent regions of solid can always feed the facet plane. Even when one of the curvatures is concave a facet does not form because new layers of solid from the adjacent region can always feed the facet plane. If there is a facet in the α-β liquid groove which runs along the lamellar plane, the presence of such facet will render the groove relatively immobile. If micro-

facets are present in the $\alpha - \beta$ liquid groove, the structure will become irregular with $\alpha - \beta$ boundary tending to follow the facet plane.[39,41]

The complex regular structure grows as a faceted cell like structure. Each facet on the cell may be regarded as a macrofacet. On each macrofacet the structure is regular. When the cell-like structures are faceted, the facet material is usually present as a skeleton almost completely surrounded by the non faceting phase, even when the non-faceted phase has the large volume fraction.

For example, the Bi-Pb eutectic alloy shows complex regular[42,43] structure having skeletal triplet[44]. A study of decanted interface shapes indicated that the interface was composed of an array of triagonal pyramid protruding into the liquid phase. The triplet formations increased in size and symmetry with decreasing growth rate and at the lowest rate used the lamellar in some triplet segments shows sign of degeneracy. On the other hand, in the Bi-Sn eutectic alloy the phases are arranged in a honey comb network[44], with a tendency towards a skeleton triplet formation. A decanted interface section indicated that these formations grew in a manner similar to those in Bi-Pb_2Bi eutectic. The analysis of the microstructure of the samples shows that there is a range of coupled growth skewed under the Bi-rich side of the eutectic.[45]

Looking at the two dimensional microstructure of a irregular or complex regular structure, the second phase particles seem to be discontinuous. However, examination with the Scanning Electron microscopy[38] shows that all the second phase particles are in fact interconnected. Etching of typical microstructure and examination

of fracture surfaces en the extracted silicon particles from the Al-Si eutectic alley revealed the presence of single and multiple twin traces. X-ray Laue photographs showed that the irregular plates were $\{111\}$ and contained $\{111\}$ twins[38]. It was the presence of these twins that gave rise to the apparently random array of silicon crystals, the crystals being interconnected and related to each other via multiple twinning operations.

Recently it has been shown that the regular rodlike $(InSb-NiSb)$[39] er broken lamellar structure $(Bi-Zn, Bi-Ag, Bi-Au)$[15,35,39,44,46,47] is formed in alleys having faceted - non-faceted phases, when the faceted phase has large volume fraction. In Ag-Bi system, the Ag rich phase is non-faceted in Ag rich melts and faceted in metals approaching the eutectic compositions, while the Bi-rich face is always non-faceted[48]. The structure of the In-Zn eutectic was found to be broken lamellar[49]. In Bi-Zn eutectic, Zn phase appears as discontinuous ribbon in a Bi phase matrix[44]. The transverse section of Bi-Ag, Sn-Zn and Pb-Ag eutectic alloys shows a perforated lamellar structure[43,50]. However the scanning electron microscopy revealed that the structure consisted of multiple branched ribbons[47].

The Al-Si eutectic forms irregular structure showing discontinuous and randomly oriented flakes of Si embedded uniformly in the Al matrix. Scanning Electron microscopy[38] has shown that the silicon flakes are not discontinuous, all the flakes being branched together. Bell and Winegard[16] have reported a structure of directionally frozen Al-Si alley containing aligned silicon crystals which grew at very slow growth rates. Further Cooksey, Day and Hellawell[27] described the same structure and showed that the

dimensions and shape of the silicon crystals are sensitive to the temperature gradient. A detailed study of all growth forms of silicon and a rationalisation of their occurrance in terms of growth rate, temperature gradient and alloy composition has been made by Day and Hellawell[51].

Using pure components (< 5 ppm total impurities) alloys in the range 12-20 wt. %$_e$ Si were directionally frozen over a range of rates from 0.1 to 10 cm/hr, with temperature gradient which varied from 0.35 to 40°C/mm. The microstructures which occurred were tabulated[51,52] into three regions A, B and C, and the limit within which they occurred is depicted in Figure 10.

Of these three regions, C includes the growth conditions which are thought to be typical of the foundry or laboratory alloy preparation, region B includes the textured silicon crystals, silicon occurring as rods. This is the region for which $G/R < 10^7$ °C sec./cm^2 Region A defines the condition within which coupled growth does not occur, here $G/R > 10^7$ °C sec./cm^2, the two phases grew from the liquid almost independently.

In the Bi-Cd eutectic alloy[44] a transverse section shows cells of regularly formed lamellar separated from each other by irregular regions. The cells are elongated in a direction parallel to the lamellar. A longitudinal section shows that the lamellar are themselves growing at a small angle to the specimen axis, the lamellar making an angle of 5-8° with the specimen axis for growth at the lower temperature gradient, and 10-14° for growth at higher temperature gradient when the cell boundaries are less marked. In the irregular regions there is also a tendency for lamellar growth to occur.
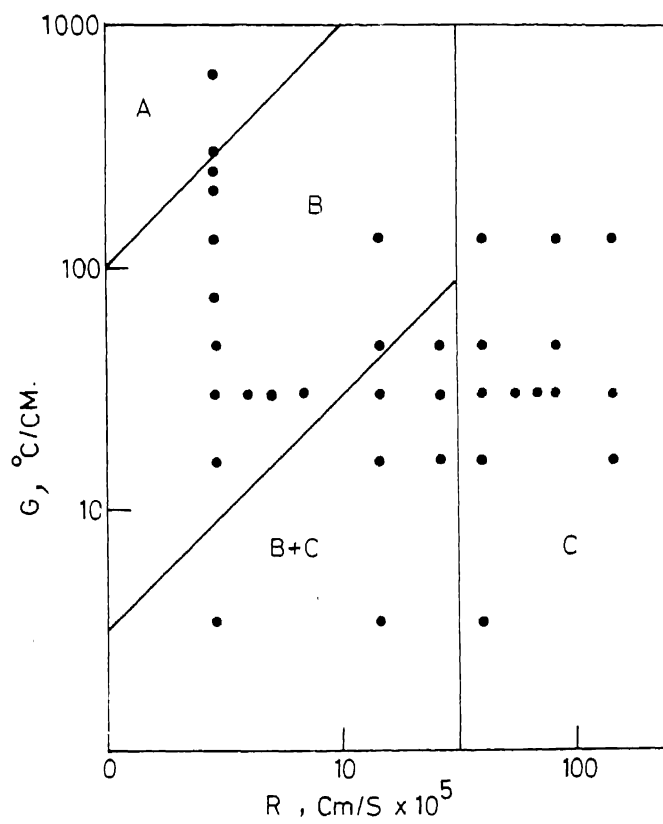
FIG.10 _ G/R PLOT FOR Al - Si EUTECTIC
ALLOYS SHOWING THE THREE
DISTINCT GROWTH REGIONS A, B & C[52]

2.5 Factors Affecting Zone Refining:

In zone refining a number of molten zones are passed through the charge in one direction. Each moving zone carries a fraction of impurities $|K < 1|$ to the end or in some cases $|K > 1|$ to the beginning of the charge, thereby purifying the remaining and concentrating impurities at one end. [53,54,55]

The efficiency of the zone refining depends upon the value of Distribution Coefficient $|K|$, which is defined as the concentration of solute |impurities| in the solid divided by its concentration in the liquid. The closer the liquidus and solidus lines the nearer to unity is the distribution coefficient, [54] thereby rendering the zone purification process impracticable. Value for K may vary from 0.001 to 10. Generally speaking, the impurities which tends to lower the melting point ($K < 1$) concentrate in the molten liquid and those raising it ($K > 1$) will tend to accumulate in the solid[54]. The distribution of impurities will depend upon the value of K as shown in Figure 11. Lower the value of K, better is the refining.

Zone refining depends upon the number of passes. As the number of passes increases the extent of purification goes on increasing till we get almost pure material. After passing the molten zone ence through an ingot we have three regions[55], (a) region of purification in which the solute concentration rises sharply from KC_o to C_o [C_o is the initial concentration of impurities in the bar], (b) a zone of levelled region of concentration C_o, (e) and a short terminal region in which the concentration exceeds C_o.

LOG CONCENTRATION OF SOLUTE IMPURITIES

5

K=5.0

K=2.0

1.0

K=0.5

K=0.1

0.1

K=0.01

0.01

0   0.2   0 4   0 6   0.8   1 0

FRACTION SOLIDIFIED

n=1
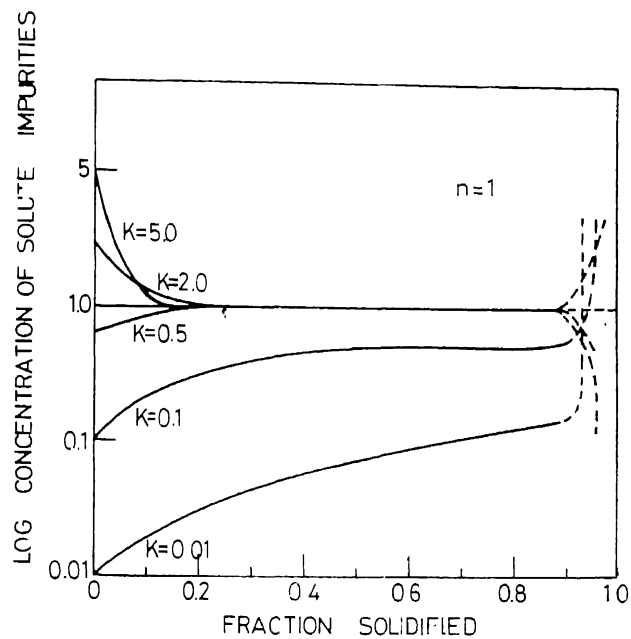
FIG 11_ CURVES FOR SINGLE PASS ZONE
MELTING SHOWING SOLUTE CONCENTRATION
IN THE SOLID Vs FRACTION SOLIDIFIED
FROM THE BEGINING OF THE CHARGE
FOR VARIOUS VALUE OF THE DISTRIBUTION
COEFFICIENT[54]

As the number of passes increases, the first region of purification increases, also the impurity concentration in this region decreases, and the zone levelled region decreases in length. Finally zone levelled region disappears. The last terminal region increases in length and also the impurity concentration increases. The distribution of impurities with different number of passes is shown in Figure 12.

A stable and compact zone with the sharpest possible demarcation between the liquid and solid phases gives the best chance of success. Such an ideal zone depends upon the degree to which it is possible to focus the heat input. It is easier to produce a narrow molten zone in a material having a high melting point and poor thermal conductivity, than in a material having a melting point near room temperature and good thermal conductivity.

Speed of travel of molten zone is also an important factor in deciding the efficiency of the refining process. For best result the speed should be such that the solid state diffusion is negligible and the diffusion is liquid is complete. However this is not practically possible. Thus the speed of zone travel must be more rapid than the rate of solid diffusion and yet not so fast as to prevent reasonably efficient diffusion of impurities into the molten zone[55] The zone speed can be increased ten times or even more for a given degree of purification, if efficient stirring of molten zone is accomplished.

The selection of suitable container material and atmosphere is very essential. The required physical and chemical characteristics of the container material are[56] (a) Inertness in relation to
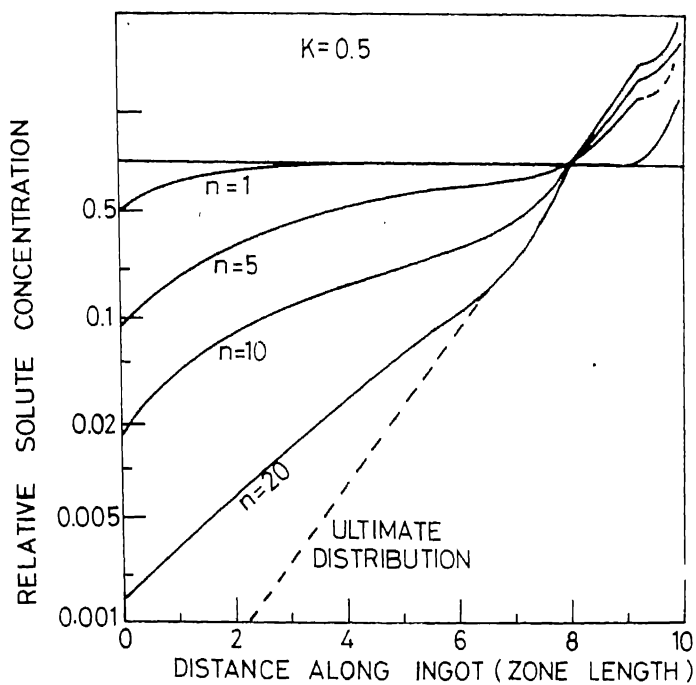
FIG.12 _ CURVES SHOWING SOLUTE CONCENTRATION
IN SOLID VERSUS DISTANCE IN ZONE
LENGTHS FOR VARIOUS NUMBER OF
PASSES[55]

the material being purified, (b) Molten material should not wet the container, (c) Thermal conductivity of the container material should be comparable to or less than that of the charge, in order to minimize heat transfer problem.

Thin walled containers offer definite advantages. Heat conductance is minimum, so a sharp molten zone is possible. Also a thin walled container can better withstand the thermal stress gradients associated with the zone refining process.

Work of different workers for zone refining of different metals, including travel speed, number of passes, atmosphere and container material is summarized in Table 5.

Table 3

Elements Purified by Zone Refining.[56]

Metal	Boat material	Source of heat	Travel speed and no. of passes	Atmosphere	Impurities	Ref.
Cd	Tantalum sheet boat	Resistance heating	1"/hr 15-30 passes	Argon	Te,Bi,Pb,Cu,Sb, Zn-K for all less than 1	57
Cd	-	-	-	Purified H_2	Purity > 99.9999	58
Zn	-	-	2"/hr 6 passes	Air	Pb,Cd reduced to 1 ppm from initial conc. of 12 ppm Pb, and 2 ppm Cd respectively. Tl and Bi effectively removed.	
Zn	Graphite or fused quartz	-	-	Purified H_2	-	
Bi	Pyrex	Induction	1.8"/hr 45 passes	Vacuum 2.5 x 10-2 mm Hg	Ag, Cu, Pb, Sn, Ni, Mg and Ca $|K<1|$ Fe $|K>1|$ Total metallic impurities < 10 ppm	59
Bi	Glass	Resistance	20 passes	Vacuum	-	60
Bi	-	-	0.5"/hr	-	Zn, Cu, Ag K<1 Sb K > 1.	
Al	Graphite	Induction	6"/hr 18 passes	vacuum 10-6 mm Hg	Cellular structure indicative of impurities present in last quarter of bar but absent in first half of bar.	61

Metal	Heat material	Source of heat	Travel speed and no. of passes	Atmosphere	Impurities	Ref.
Al	Graphite	Induction	4,9"/hr. 20 passes	Argon	-	62
Al	Graphite	-	30 passes	Argon	Purity increased from 99.992 to 99.9995	63
Sn	Alumina or Quartz	-	8"/hr 50-60 passes	Air	Sb,Ca and Mn (K>1), Pb,Cu, Bi,Cd,Fe,Ag,In,Zn,Au,Ni,Al, Mg,and Si (K<1) Si,Al and Fe Most effectively removed purity > 99.999	64
Sn	Graphite	-	2"/hr a passes	Argon	-	
Sn	Pyrex	-	40 passes	Vacuum	99.9 percent Sn converted to 99.9999 purity	65
Sn	Pyrex Quartz or graphite	-	2"/hr 500 passes	Argon	Most impurities below limit of detection exceptions are Al,Cd,Fe,Mg,Si and Sb.	
Sb	-	-	7 passes	H$_2$	Ni,Pb,Ag and Cu reduced by factor of 10. As (K>1) not removed.	65
Sb	Graphite	-	25 passes	-	-	
Pb	Vycor tube coated with a film	Induction	-	Argon	-	66

CHAPTER 3

MATERIALS AND EXPERIMENTAL PROCEDURE

3.1 Formulation of the Problem:

The literature review reveals that the classification of eutectic alloys proposed by different workers is neither full proof nor complete. There are some alloys which, according to one classification are regular while according to the other irregular or complex regular |See Table 3|. It has also been shown by some workers[6,8] that irregular or complex regular structure is not the inherent property of that particular system, and that the system which solidifies as irregular or complex regular structure can be made to solidify as regular structure[28] by using high purity (zone refined) metals and controlled rate of solidification[28].

For the present work it was decided to choose the systems which shows irregular or complex regular structure according to one or another classification. Few alloys which were difficult to classify easily have also been included. Form of these alloys according to one classification should be regular while on the basis of the other irregular. It was decided to zone refine the alloy itself, instead of zone refining the individual components. The advantages of zone refining the alloys are (a) any proeutectic component, if present, will segregate in the first part of the bar[67], (b) those impurities, which have K values very much less than one for one component and nearly equal to or slightly above one for other component, can also be removed efficiently. The only impu

which has K value less than one for one component and much greater
than one for the other component is really difficult to remove,
(c) the actual amount of work involved is considerably reduced.

The zone refined alloy was then zone levelled and finally
given the directional solidification pass at a given slow speed.
Then the microstructures in relation to the growth direction were
studied to examine the results.

3.2 Material and Equipment:

The phase diagrams of the binary eutectic alloy systems,
Pb-Sb, Bi-Cd, Zn-Sb, Bi-Pb, Bi-Sn, Bi-Zn and Sn-Zn, examined are
given in Figures 13 and 14. The metals used for making the alloys
had better than 99.9 percent purity. The zone refining was done
in purified argon so as to prevent oxidation of the metal. Initially
the graphite boat was used for the purpose. However, a very wide
molten zone was obtained since graphite is very good conductor of
heat. A sharp and confined molten zone was obtained by using
quartz which is a relatively poor heat conductor.

The heat source for melting was a resistance furnace, made
up of a single coil Kanthal A, 16 gauge wire. The Kanthal wire was
coiled as a 12 mm diameter coil and fixed up in a fireclay brick
having a hole of 37 mm diameter. The brick was surrounded by the
two copper plates in which groves were made for water circulation.
The circulating water ultimately cooled the copper plate and helpe
in getting a sharp molten zone.

The apparatus used for zone refining had the arrangement fo
moving the furnace at the desired speed between 2.0 to 50 cm/hr in

I Pb - Sb

II Bi - Cd

III Zn - Zn₃Sb₂

IV Bi - Pb
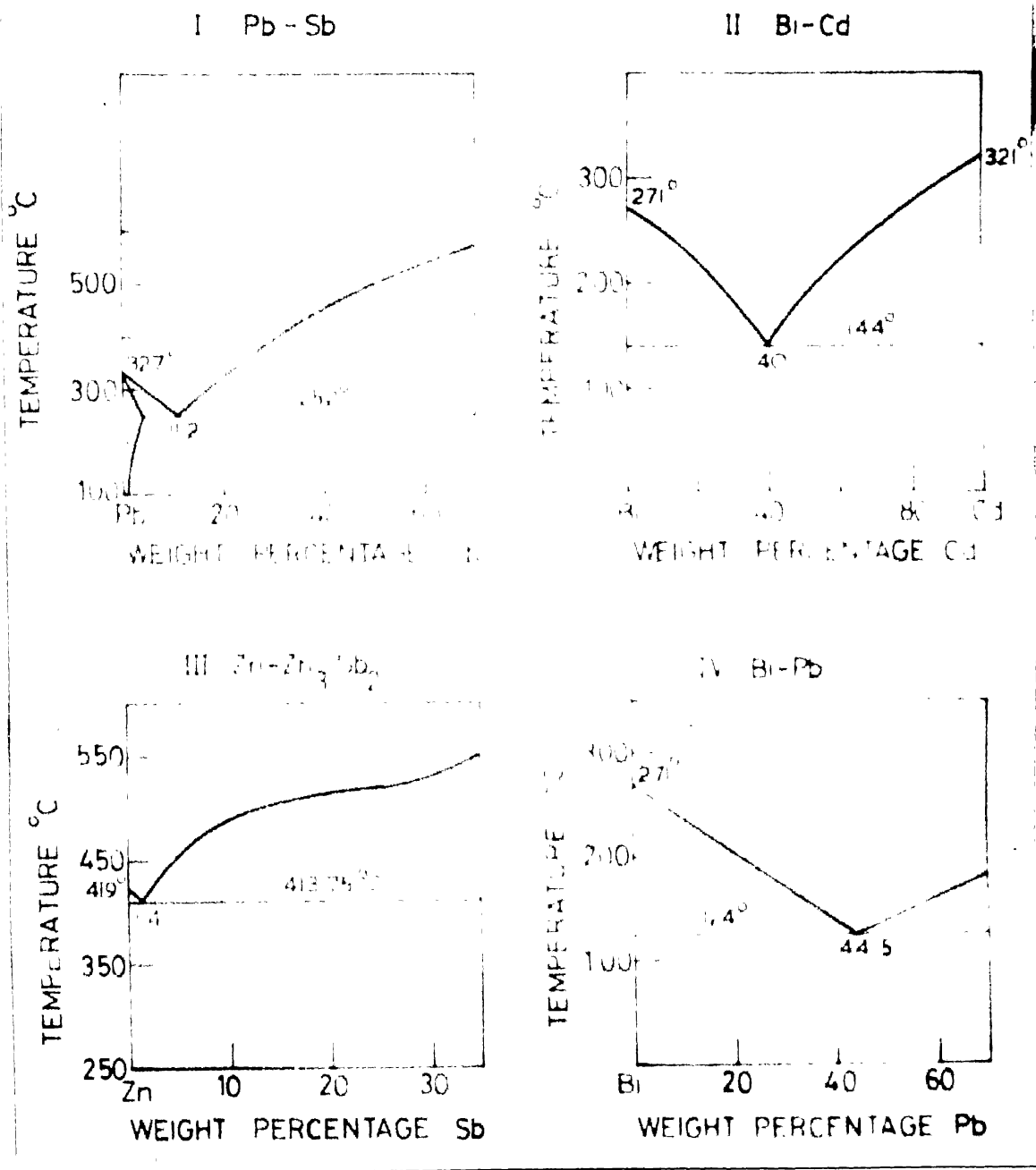
FIG - 13   PHASE DIAGRAMS ⁶⁸

V Bı - Sn
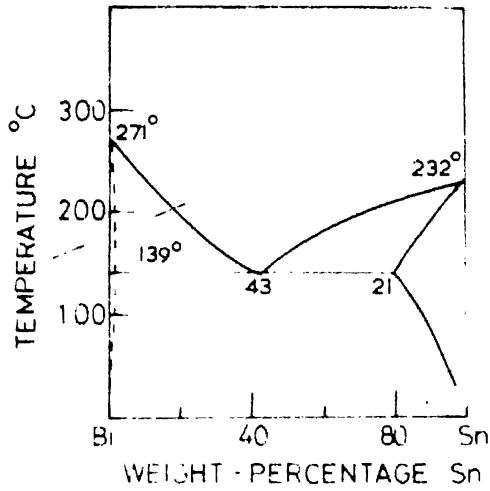
VI Bi -Zn
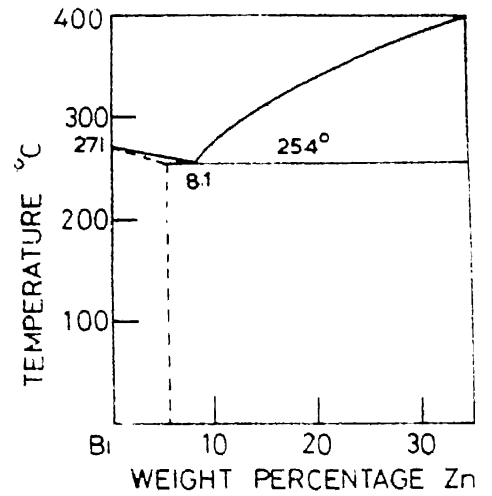
VII Sn-Zn
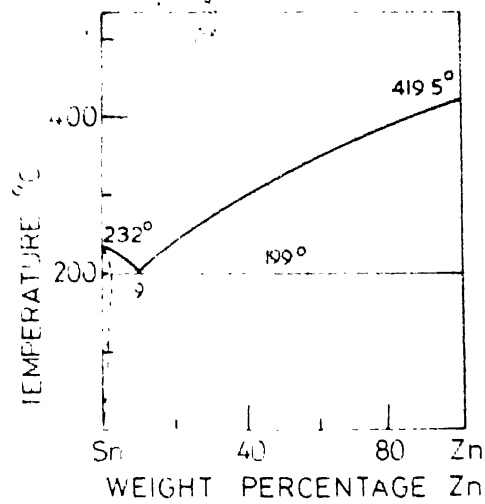
FIG.14_ PHASE DIAGRAMS[68]

forward direction and comparatively rapidly in the backward direction when set for zone refining. The very slow speed of the furnace motion could be chosen when set for some levelling work. The L & N Electromage controller was used to control the temperature of the furnace.

3.3 Experimental Work:

The alloys were melted in vacuum sealed 12 mm diameter pyrex tubes to give bars of the same size, which were then swedged down to the 6.25 mm diameter size bars. For making alloys of Bi-Cd Bi-Zn and Bi-Sn, the melting was done in tubes of 6.25 mm diameter to give the final rods, because of the brittle nature of the alloys

For zone refining the furnace was set at a particular temperature and the bar was kept in the cleaned quartz boat. After the furnace had attained the steady state it was allowed to move with the required speed of 75 mm/hr. The outer temperature was so adjusted that the actual zone width in the boat was about 20 mm. If zone width was more it could be reduced by decreasing the furnace temperature.

Different speeds and different number of passes have been used by different workers[56]. For the present work it was decided to zone refine the metal at the speed of 75 mm/hr using 5, 10 and 25 zone refining passes. After zone refining, each bar was cut from both ends. One inch from the starting end and two inches from the last end. The remaining middle part of three inches length was zone levelled at the speed of 75 mm/hr for three times each way [forward and backward], finally the zone levelled bar was directionally solidified at the rate of 20 mm/hr, which was the minimum speed

available with the present apparatus. Also one unrefined sample was solidified directionally for comparative study.

It was assumed that after five zone refining passes some impurities were removed which segregated in the last part, which was actually chopped off. So after some levelling the total impurity content was lower than that of the unrefined bar, and the extent of purification was increased with higher number of zone refining passes, i.e. 10 and 25 passes, so the total impurity content of the bar decreased. Hence whatever change observed in microstructure by increasing the number of passes were due to decrease in impurities of the bar.

After zone refining, levelling and slow growth passes, three samples, in relation to growth direction transverse, vertical longitudinal and horizontal longitudinal sections - were taken from the middle portion of each bar. These specimens were then ground, polished and examined under optical microscope.

As the alloys were quite soft, it was a problem to polish them and get a satisfactory scratch-free surface. For Pb-Sb and Bi-Pb alloys soap solution having alumina powder in suspension was used for polishing work. The structure was obtained directly after polishing without the use of any etchant. On the other hand for Bi-Cd, Zn-Sb, Bi-Sn, Bi-Zn and Sn-Zn alloys, the polishing was done using alumina powder in distilled water and the polished specimen was etched using following etchants:

	Alloy	Etchant
(a)	Bi – Cd	Iodine – 1 part
	Bi – Sn	KI – 3 parts
	Bi – Zn	Water – 10 parts
(b)	Zn – Sb	Cr_2O_3 200 gm.
		Na_2SO_3 15 gm.
		Water 1000 ml.
(c)	Sn – Zn	Nital

Finally, the representative microphotographs were taken
for each alley and the results interpreted.

RESULTS

I. PbrSb:

The schematic microstructures are shown in Figure 15 and microphotograph of the random distribution in Figure 16. The as cast structure showed the random distribution of the second phase particles which were flakey in nature. After some refining and directional solidification the structure becomes coarser, with the slight tendency of the flakes to orient in the direction of growth. No remarkable change was observed in this system.

II. Bi-Cd:

The schematic microstructures are shown in Figure 17 and microphotographs in Figure 18. The as cast structure shows the grains having different orientations of the second phase particles. The second phase particles are elongated and curly in nature. The structure was cellular as characterized by alternating coarse-fine arrays of the second phase.

After slow growth pass in the unrefined state the grains disappear but the structure is still cellular (Figure 18(a)). The second phase particles, which were still curly, have tendency to orient in the direction of growth (Figure 18 (b)). Transverse sect: shows that these second phase particles make an angle with the ver tical. Overall structure seems to be coarser than the as cast one (Figure 18(b)).

I Pb-Sb
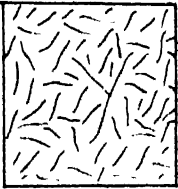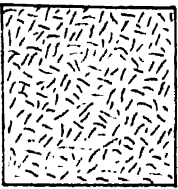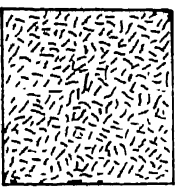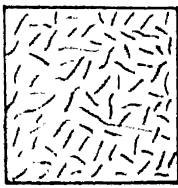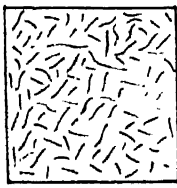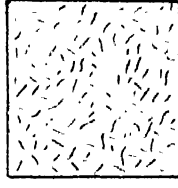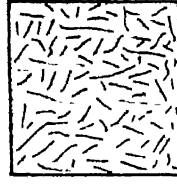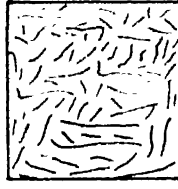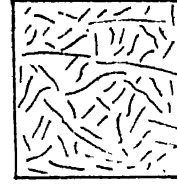
SECTION NO. OF PASSES	TRANSVERSE	VERTICAL LONGITUDINAL	HORIZONTAL LONGITUDINAL
ZERO			
FIVE			
TEN			
TWENTY FIVE			

FIG15_ SCHEMATIC MICROSTRUCTURE (DARK PHASE_Sb)
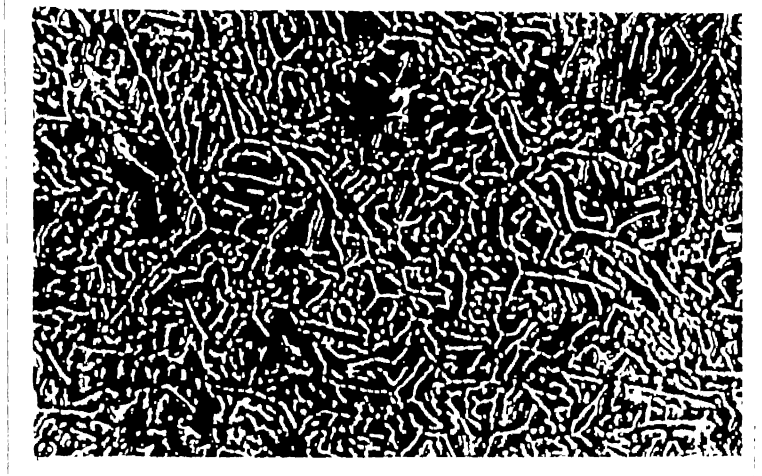
Transverse section (Bright phase Sb)

X 450

Fig. 16: Lead - Antimony Alloy.

II Bi-Cd
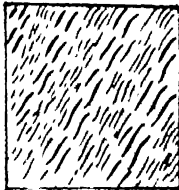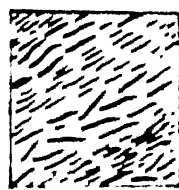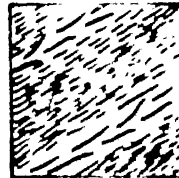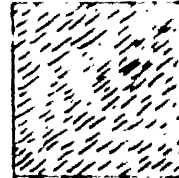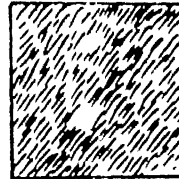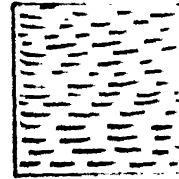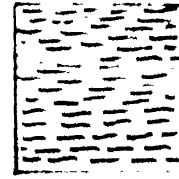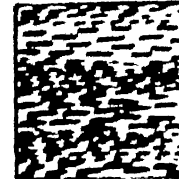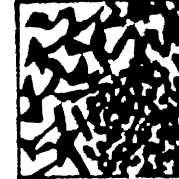
SECTION NO. OF PASSES	TRANSVERSE	VERTICAL LONGITUDINAL	HORIZONTAL LONGITUDINAL
ZERO			
FIVE			
TEN			
TWENTY FIVE			

FIG 17 SCHEMATIC MICROSTRUCTURE (DARK PHASE Cd)

(a) Transverse section
    unrefined X 600

(b) Vertical longitu-
    dinal section –
    unrefined X 600

Fig. 18: Bismuth – Cadmium (Dark phase Cd).

After five zone refining passes, the second phase particles are less curly, having better orientation in the direction of growth. The cellular structure still persist. In transverse section the angle which the second phase particle makes with the vertical direction, seems to be larger as compared to the previous case.

As the number of passes increases, the structure becomes more uniform, the second phase particles less curly and better oriented in the direction of growth. The transverse section after twenty five passes shows that the second phase particles are oriented in the horizontal direction (Figure 18(e)). The gradual alignment of the second phase in the transverse section with zone refining is particularly remarkable. The horizontal longitudinal section shows irregular shaped and inter-connected second phase particles with coarse and fine regions (Figure 18 (e)). A comparison of the horizontal longitudinal section with the transverse section indicate the actual shape of the particles, which are in the form of plate-l
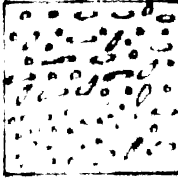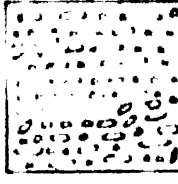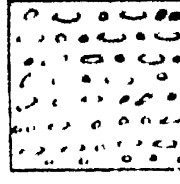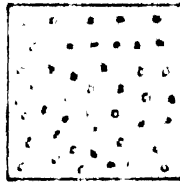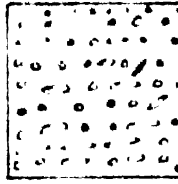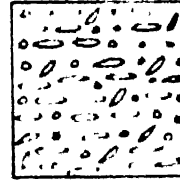
III. Zn-Sb:

The schematic microstructures are shown in Figure 19 and some representative microphotographs in Figure 20.

The as cast structure is non-uniform and the distribution of the second phase particles which appeared to be elongated were random. After the slow growth pass of unrefined bar, the distribution is still random with second phase particles of varying size and shape (Figure 20(a)).

After five zone refining passes the second phase particles shows tendency to orient in the direction of growth. In transverse section the particle shape is almost circular (Figure 20(b)), while

III Zn - Sb

SECTION No. V PHASE	TRANSVERSE	VERTICAL LONGITUDINAL	HORIZONTAL LONGITUDINAL

(DARK PHASE Zn_3Sb_2)

(d) Transverse section
    -after 25 Zone
    refining passes,
    X 300.

(e) Vertical longi-
    tudinal section
    after 25 Zone
    refining passes,
    X 300.
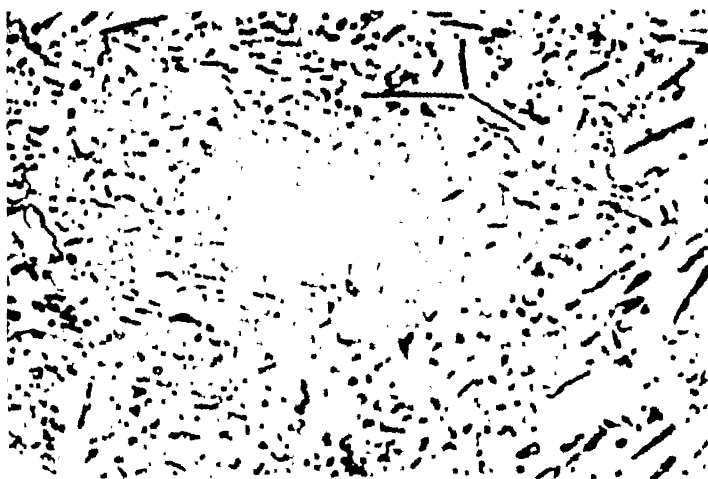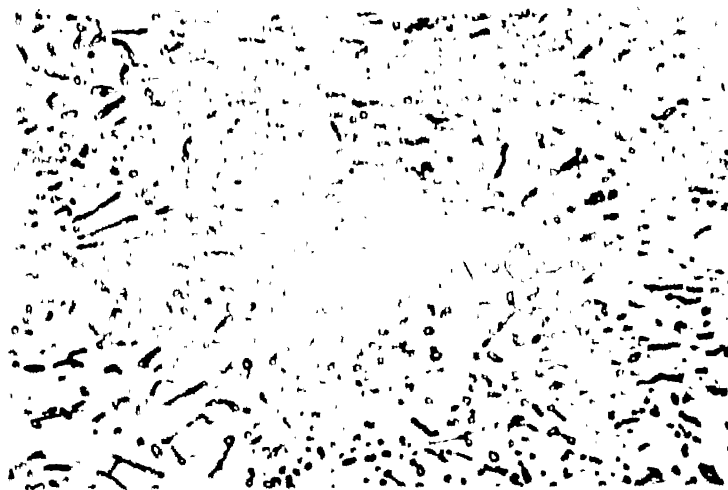
(f) Horizontal longitu-
    dinal section -
    after 25 Zone
    refining passes, X 300.

Fig. 20 (Contd.): Zinc - Antimony (Dark areas Zn_3Sb_2).

ongitudinal sections shows both circular and elongated particles.
ence it would appear that the shape of the second phase particles
aried from spherical to broken rods.

As the number of passes increases, the structure becomes more
and more uniform and the elongated particles shows better tendency
to orient in the direction of growth (Figure 20(d,e,f)).

IV. Bi-Pb:

The schematic microstructures are shown in Figure 21 and some
microphotographs in Figure 22. Complex regular structure was observed
in the as - cast structure having regular regions of triplets and
irregular structure between the triplets. The triplets were randomly
oriented. After slow growth pass of unrefined bar, the structure
was yet random and seemed to be somewhat finer (Figure 22 (a) and (b)).

After five some refining passes the structure became coarser
(Figure 22(c)). The longitudinal section showed that the triplets
had a tendency to orient in the direction of growth. The structure
between the triplets was still random. As the number of passes
increased, the second phase particles between the triplets tended
to orient in the direction of growth (Figure 22 (d) and (e)).

V. Bi-Sn:

The schematics of microstructure are shown in Figure 23 and a
few representative microphotographs in Figure 24. The complex regular
structure, honeycomb and random distribution of the second phase in
between honeycomb, was observed in the as-cast structure. The fans
were randomly oriented. After slow growth pass, in unrefined state,
fans had a slight tendency for vertical orientation in transverse

Ⅳ Bi-Pb
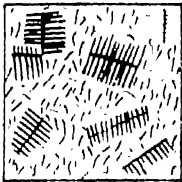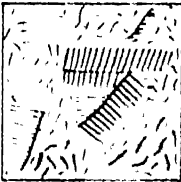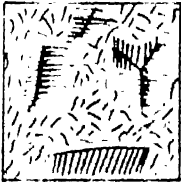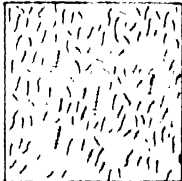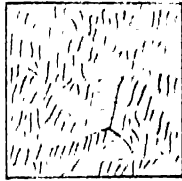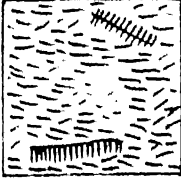
SECTION NO. OF PASSES	TRANSVERSE	VERTICAL LONGITUDINAL	HORIZONTAL LONGITUDINAL
ZERO			
FIVE			
TEN			
TWENTY FIVE			

FIG 21 _ SCHEMATIC MICROSTRUCTURE (DARK PHASE . Bi)

(a) Transverse section-unrefined, X 450.

(b) Vertical longitudinal section-unrefined, X450.
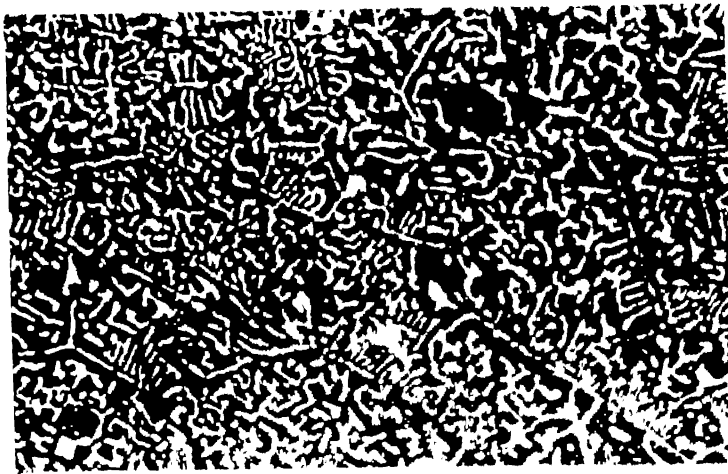
(c) Transverse section -after 5 Zone refining passes, X 450.
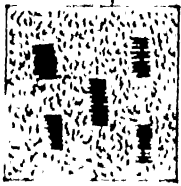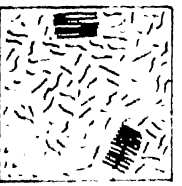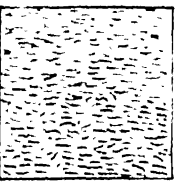
Fig. 22: Bismuth - Lead (Dark Phase Pb_2Bi).

$\underline{\mathrm{V}}$ Bi-Sn
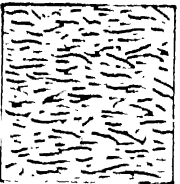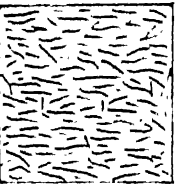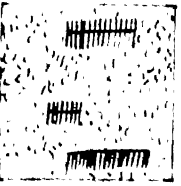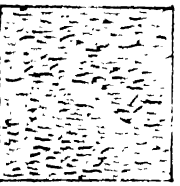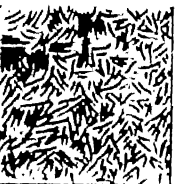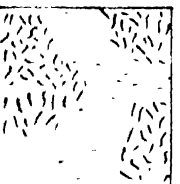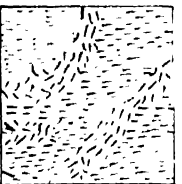
SECTION NO. OF PASSES	TRANSVERSE	VERTICAL LONGITUDINAL	HORIZONTAL LONGITUDINAL
ZERO			
FIVE			
TEN			
TWENTY FIVE			

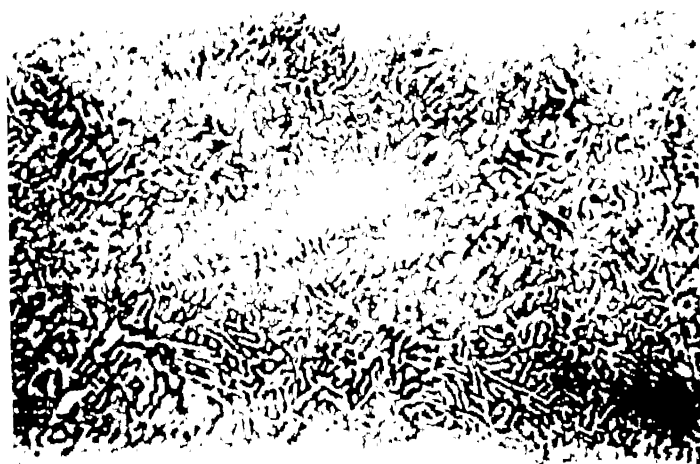FIG 23. SCHEMATIC MICROSTRUCTURE (DARK PHASE - Bi)

(a) Transverse section
    -unrefined, X 600.

(b) Vertical longi-
    tudinal section
    unrefined, X 600.

(c) Vertical longitud
    section - after
    5 Zone refining p.
    X 600.

Fig. 24: Bismuth – Tin (Dark phase – Bi).

(d) Transverse section
after 25 Zone
refining passes,
x 600.

(e) Horizontal longi-
tudinal section-
after 25 zone
refining passes,
X 600.

Fig. 24 (Contd.): Bismuth – Tin (Dark phase – Bi).

on (Figure 24 (a)), and to orient in the direction of growth
ngitudinal section (Figure 24 (b)). Overall structure was still
n.

After five zone refining passes the structure became coarser
less fans and the second phase particles showed tendency to
it in the direction of growth (Figure 24(c)). Second phase parti-
were curly in nature. As the number of passes increased, the
r of fans decreased, and the second phase particles had better
ency to orient in the direction of growth. Second phase particles
less curly. The transverse section after twenty five zone refin-
passes showed random orientation (Figure 24(d) while longitudi-
section showed orientation in the direction of growth with some
me and fine regions (Figure 24 (e)).

Bi-Zn:

The schematic microstructures are shown in Figure 25 and a few
resentative microphotographs in Figure 26. The as cast structure
red grains having different orientation of the second phase par-
les. After slow growth pass of unrefined bar, the grain boundaries
e still evident in the transverse section (Figure 26(a)). The
gitudinal section showed that the second phase particles were
ented in the direction of growth and had mildly corrugated struc-
e in the horizontal longitudinal section. An accentuated corru-
ion was occassionally observed, the typical example of which is
wn in Figure 26 (b) .

After five zone refining the grain boundaries disappeared, the
ucture was coarser then the previous one. In the transverse section
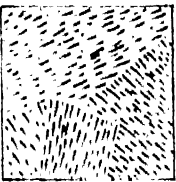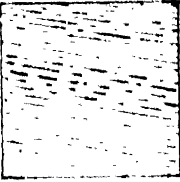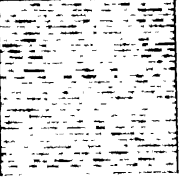second phase particles were oriented at an angle to the vertical

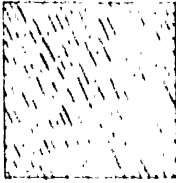## $\overline{\text{VI}}$ Bi – Zn
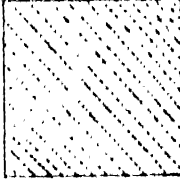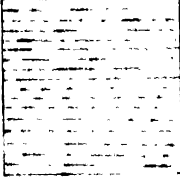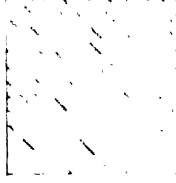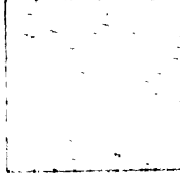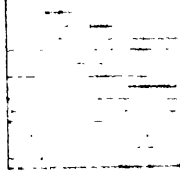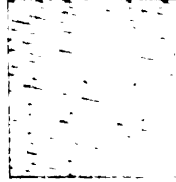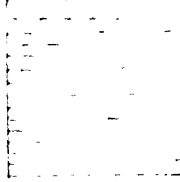
SECTION NO. OF PASSES	TRANSVERSE	VERTICAL LONGITUDINAL	HORIZONTAL LONGITUDINAL
ZERO			
FIVE			
TEN			
TWENTY FIVE			

FIG. 25 _ SCHEMATIC MICROSTRUCTURE (DARK PHASE _ Zn)
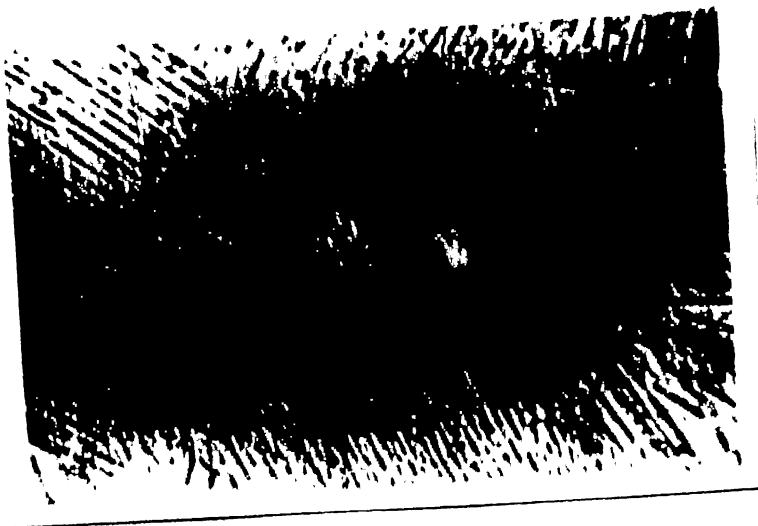
(a) Transverse section – unrefined , X 600

(b) Horizontal longitudinal section – un-refined, X 600
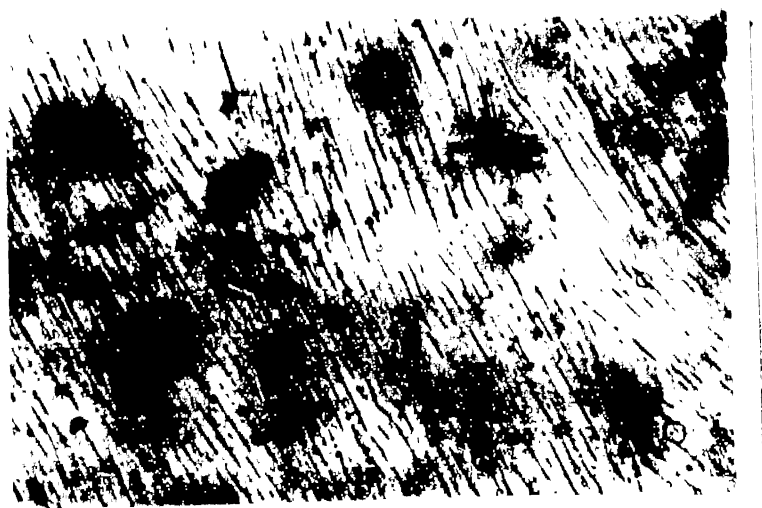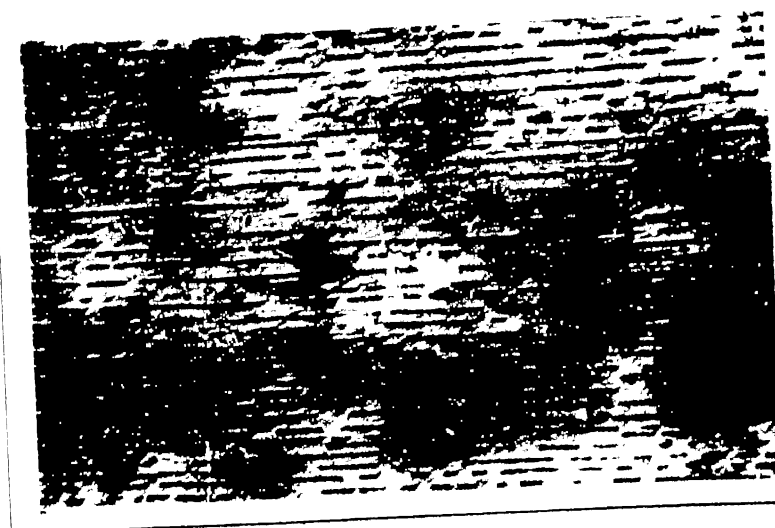
(c) Transverse section – after 5 Zone refin-ing passes, X 600

Fig. 26: Bismuth – Zinc (Dark phase Zn).
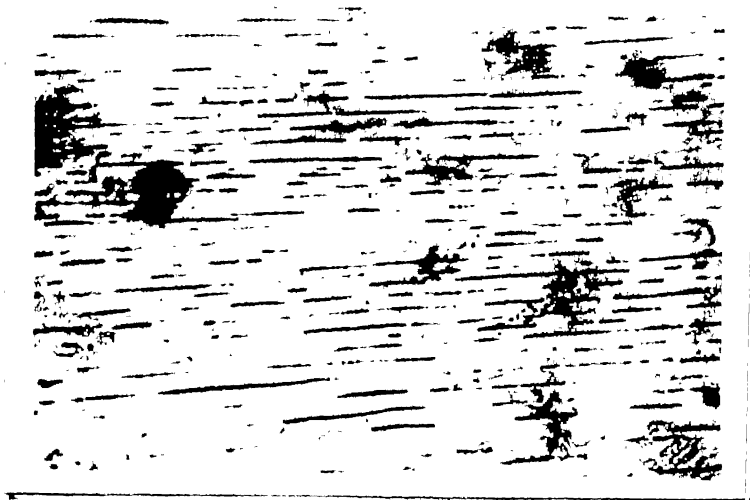
(d) Horizontal longitu-
    dinal section –
    after 10 Zone
    refining passes,
    X 600

(e) Transverse
    section – after
    25 Zone refin-
    ing passes,
    X 600

(f) Vertical longitudinal
    section – after 25
    Zone refining passes,
    X 600.

Fig. 26 (Contd.): Bismuth – Zinc (Dark phase Zn).

(figure 26(c)). In longitudinal section they were not oriented
in the direction of growth. As the number of passes increased, the
orientation of the second phase particles in transverse section
tends to become horizontal (Figure 26 (e)). The longitudinal section
showed tendency to become continuous and oriented in the direction
of growth (Figure 26 (d) and (f)).

VII. Sn-Zn:

The schematic microstructures are shown in Figure 27 and a
few representative microphotographs in Figure 28. The as cast
structure showed the second phase particles in the form of broken
lamellar. After slow growth pass of the unrefined bar, the trans-
verse section had some grains, having coarse and fine regions (Figure
28(a)), each grain having a distinct orientation of the lamellar
array. The vertical longitudinal section showed both elongated and
circular cross sections of the second phase particles, without align-
ment in any particular direction. The horizontal longitudinal sec-
tion showed fine elongated particles aligned in the direction of
growth and some circular sectioned particles in the form of humps
distorted in the direction perpendicular to that of growth (Figure 28(b

After 5 some refining passes, the transverse section still had
grain structure. The longitudinal section showed elongated disconti-
nuous particles, oriented in the direction of growth (Figure 28c).
As the number of passes increased, the structure became finer in the
transverse section. The grain boundaries were still evident, where
as the second phase particles varied between the circular and elongate
in shapes (Figure 28 (e)). The longitudinal section showed better alig
ment in the direction of growth and the tendency of the second phase
particles to become continuous (Figure 28(d)).

VII Sn-Zn
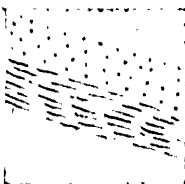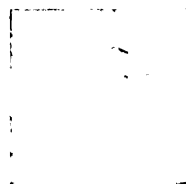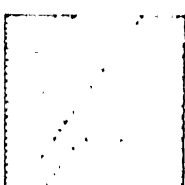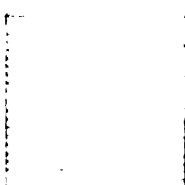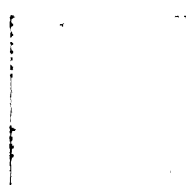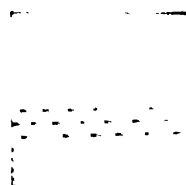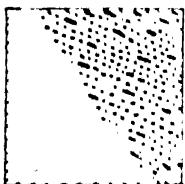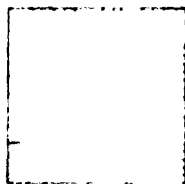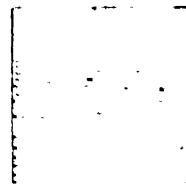
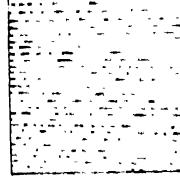| SECTION NO. OF PASSES	TRANSVERSE	VERTICAL LONGITUDINAL	HORIZONTAL LONGITUDINAL
ZERO			
FIVE			
TEN			
TWENTY FIVE			

FIG 27 — SCHEMATIC MICRO STRUCTURE OF Sn-Zn
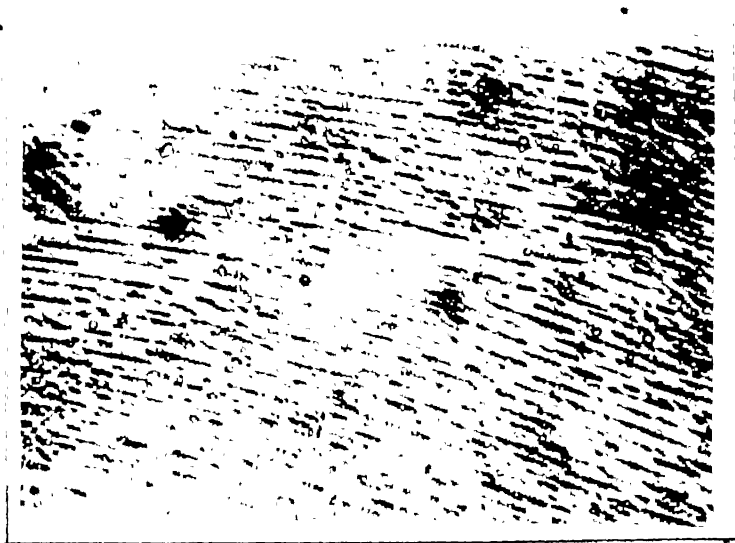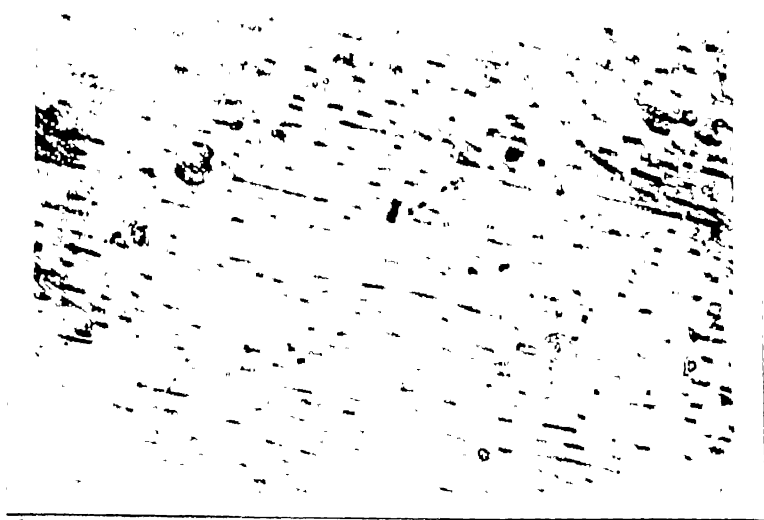
(a) Transverse Section –
    unrefined, X 900

(b) Horizontal
    longitudinal
    section –
    unrefined, X 900
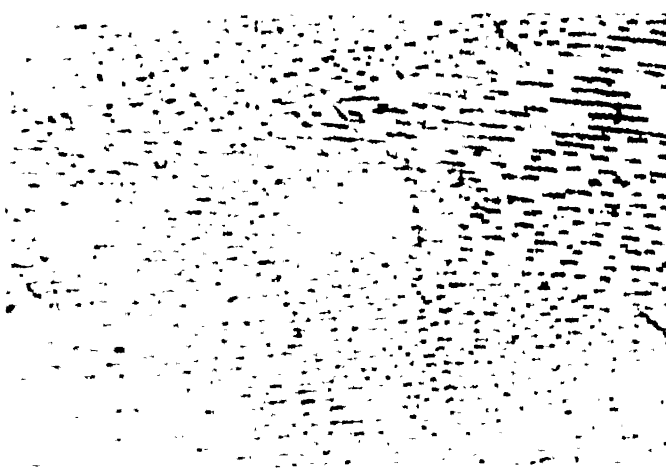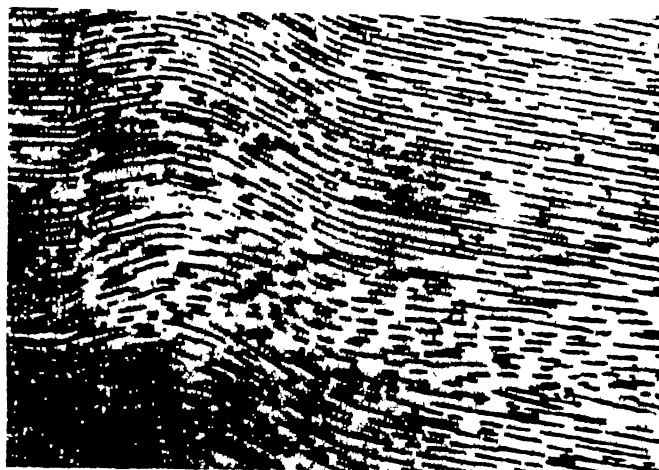
(c) Vertical longitudinal
    Section – after 5 Zone
    refining passes, X 900

Fig. 28: Tin – Zinc (Dark phase Zn).

(d) Vertical Longitudinal
    Section – after
    10 Zone refining
    passes , X 900

(e) Transverse
    Section – after
    25 Zone refining
    passes , X 900

Fig. 28 (Contd.):   Tin – Zinc (Dark Phase Zn).

CHAPTER V

DISCUSSION

The structure observed in the case of Bi-Cd eutectic alloy seems to be similar to that produced in the regular (lamellar) eutectics by the presence of impurities[44]. The growth takes place in two preferred directions, making different angles with the normal to the surface. The higher growth rate makes larger angle with the normal to the surface, while the slower growth rate makes smaller angle with the normal, so that they are able to keep pace during growth.[11]

Cells of regularly formed lamellar separated from each other by triangular regions, were initially oriented at an angle to the vertical [P.S], and as the impurity content decreases, these cells orientation tends to become horizontal, also the number of cells decreases with decrease in impurity content, the similar effect has been observed by decreasing growth rate[44].

Three dimensional form can be interpreted by comparing the three sections after twenty five passes, which shows that the second phase particles [Cd phase] are interconnected and in the form of platelets. These platelets are of varying size and shape. Bigger size platelets corresponds to the coarse region and smaller ones for fine region of cellular structure. The platelets are interconnected in the plane of the platelets. The interconnection of the coarse and fine platelets verifies that the growth changes[11] easily between the two growth directions

Second phase particles $[Ba_3Sb_2]$, of varying shape and size were randomly distributed in the parent matrix (Bn), in the impure alloy. As the impurity content decreases the second phase particles tends to acquire regular shape and those which are elongated tries to orient in the direction of growth, giving a structure corresponding to the broken fibers. Here the structure which was purely irregular tends to become more and more regular as the impurity content decreases.

A complex regular structure, having regular triplets or honey comb of Bi and an irregular region was observed in impure $Bi-Pb_2Bi$ and Bi-Sn eutectic alloys. Quenched interface shows that the complex regular structure results from the central Bi plate projecting into the liquid[15]. Such a interface has some resemblance to a dendritic structure, which forms due to supercooling of the liquid ahead of the growing interface[44]. The region without the central Bi plate are macroscopically flatter and results in the irregular region[15].

Now as the impurity content decreases the number of triplet also decreases, showing that there are less protuberances on the growing solid liquid interface. This means that as the impurity content decreases the super cooling ahead of the solid liquid interface decreases.

In the case of Bi-Sn eutectic, the irregular structure showed tendency to orient in the direction of growth, while it was difficult to say so in the case of $Bi-Pb_2Bi$ eutectic. The reason may be either the purification was not sufficient enough to give regular structure or the growth rate was high. It was quite clear that both the alloys

which were complex regular have tendency to orient in the direction
of growth, i.e. changing towards a regular structure.

The so called broken lamellar structure was observed in case
of Bi-Zn and Sn-Zn eutectic alloys. Scanning Electron microscopy
has shown that in case of Pb-Ag which is also a broken lamellar in
two dimensional microstructure, the minor phase had the branched
ribbon structure.[47] Since the branching occurred only in the plane
of the original ribbon, any microsection, except one taken through
the plane of the ribbons would have a microstructure similar to
the broken lamellar.

In the case of Bi-Zn the structure remained broken lamellar
even after purification. As the impurity content decreases the
lamellar tries to become more continuous and better oriented in the
direction of growth. Less broken structure shows that there was
less branching, so as the impurity content decreases the chance of
branching also decreases.

In the case of Sn-Zn, the second phase [Zn phase] which is in
the form of branched ribbons becomes longer in the longitudinal
section and thin in transverse section, as the alloy is purified.
The structure of purified alloy in transverse section shows more
rods and fewer ribbons. These rods did not have the regular hexa-
gonal distribution of rods found in normal rodlike eutectic and tends
to form rows of rods. Similar rods had been observed in Pb-Ag system
by Southin and Jones.[47] Scanning electron microscopy revealed
that the rods were branched in a similar manner to the ribbons, and
this accounts for the fact that the rods occurred in rows.

No great change has been observed in the case of Pb-Sb eutectic alloys except that the second phase (Sb) particles increases in size as the impurity content decreases. The general nature of the structure remained the same. This shows that either the purification is not sufficient enough or growth rate is fast to give regular structure and the structure remained completely irregular.

Considering the conditions which favour regular eutectic, it has been shown that in a lamellar eutectic there is a characteristic orientation relationship between adjacent phases.x Also there are some orientation of the planer lamellar surfaces which have low energy than others, and these lamellar arrangement are correspondingly stabilised, and such optimum orientations of the lamellar planes are called 'coincident interface'.[7] In the presence of impurities either the interfacial energy will increase or this low energy plane will not coincide with the freezing direction, making the alloy irregular.

The structure of eutectic alloy strongly depends upon the free energy of the phases, and the structure will be regular if the free energy of the two phases are nearly same, and irregular when they are very different.[15] Hence the presence of impurities will increase the difference between the free energy of the two phases. Also as shown by Davies[11], the structure will be irregular if the lead of one phase over the other is large. The effect of purification may be that the lead distance will decrease as the impurity content decreases.

An important consideration for the irregular eutectic is the energy of twin formation.[38] When energy of twin formation is low i.e.,

there is frequent twinning, the structure will be highly branched
and hence irregular. The presence of impurity might be favourable
for twinning to occur. As the impurity content decreases, the
energy for twin formation increases, making it difficult for
branching to occur, resulting in a more regular structure as is
shown in Bi-Zn and Sn-Zn systems.

The growth twins have been observed in silicon and germanium.[69]
A small driving force is necessary for twin formation and is provided
by undercooling ahead of the interface. When the undercooling is
small and is constitutional in nature (i.e. due to impurities),
instead of cells twins appear at the interface.[70] This seems spe-
cially true in materials with a strongly preferred growth direction
(which in turn may be due to faceting) to make the axis of growth
nearer to the preferred direction.

The growth twins, which are quite distinct from and unrelated
to the deformation twins, provide an array of reentrant corners to
allow rapid growth.[71] It must be emphasised that even in pure Si and
Ge, the growth twins are encountered below certain critical G/R
value.[70] For low G/R, the interface shape becomes concave to the
melt in order to develop a driving force for growth due to small
undercooling. The twin appear, the lamellar twins at low curvature
and the growth twins at high curvature, thus it would seem that
extreme reduction in impurity content and/or reduction in the growth
rate and increase in temperature gradient would stimulate twinning.

It is apparent from the undercooling data in Table 1 that
Bi, Sb, Ph_2Bi and Zn probably act as nucleants during eutectic

solidification. However, this fact does not seem to have signifi-
cance to the alignment of second phase in the Pb-Sb, Bi-Pb and Bi-
Sn eutectic alloys. The most remarkable alignment is to be found
in Bi-Cd and Sn-Zn eutectic alloys where there is a definite
orientation relationship between the two phases (See Table 2),
the Bi-Zn and Zn-Sb alloys also exhibit marked realignment. Although
no orientation data are available for these two alloys, the former
has the broken lamellar structure and is presumably similar to the
Sn-Zn alloy whereas the latter has a broken rodlike structure which
upon zone refining becomes simultaneously aligned and spheroidal
in shape. No ready explanation is forthcoming for this behaviour.

In general, the second phase alignment in all alloys is most
probably connected with the slow growth rate and with the reduced
incidence of twinning after zone-refining.

CHAPTER VI

CONCLUSION

Structure observed showed some change in five systems out of seven alloys studied. The results can be concluded as:

(a)   As the impurity content decreases the supercooling ahead of solid liquid interface decreases making the interface more planer (Bi-Sn and Bi-Pb eutectics).

(b)   As the impurity content decreases the energy for twinning increases, resulting in less twinning hence more regular structure (Bi-Zn, Sn-Zn).

(c)   The impurities have significant effect on the characteristic orientation relationship between adjacent phases, as the impurity content will decrease, the coincident interface will coincide with the freezing direction making the structure more regular.

(d)   Impurities also will change the interfacial energy of the two phases. The presence of impurities will increase the interfacial energy making the structure irregular.

(e)   The second phase alignment in all alloys is most probably connected with the slow growth rate. It is expected that using still slow growth rates (of the order of 1 mm/hr) all the alloys will have regular structure.

Considering the above points it may be concluded that the irregular structure is not the inherent property of the alloys. The structure depends upon the growth conditions and impurity contents, and all the alloys can be made to solidify in regular structure by using high purity metals and suitable growth conditions.

REFERENCES

1. Chadwick, G.A., Progress in Material Science, 12 (No.2) (1963).

2. Chalmer, B., Principal of Solidification.

3. Tiller, W.A., Liquid Metals and Solidification, A.S.M. Publication (1958), 276.

4. Collins, W.T., Jr. and Mondolfo, L.F., Trans. AIME 233 (1965), 1671.

5. Hogan, L.M., J. of Aust. Inst. of Metals., 9 (1964), 228.

6. Chadwick, G.A., J. of Inst. of Metals, 91 (1962/63), 298.

7. Cooksey, D.J.S., et.al., Phil. Mag. 10 (1964), 745.

8. Mondolfo, L.F., J. of Aust. Inst. of Metals, 10 (1965), 169.

9. Sundquist, B.E., and Moldolfo, L.F., Trans. AIME, 221, (1961), 157

10. Sundquist, B.E., Bruscato, R., and Mondolfo, L.E., J. of Inst. of Metals, 91, (1962-63), 204.

11. Davies, V. de L., J. of Inst. of Metals, 93 (1964), 10.

12. Davies, V. de. L., J. Inst of Metals, 94 (1966), 192.

13. Hunt, J.D., and Jackson, K.A., Trans. AIME, 236 (1966), 843.

14. Filonoko, V.A., Physics of Metals and Metallography (1970), 641.

15. Bagg, K.V., and Winegard, W.C., J. Phys. Chem. of Solids Suppl. No. 1 (1967), 179.

16. Bell, J.A.E., and Winegard, W.C., J. Inst. of Metals, 93 (1964-65), 318.

17. Bell J.A.E., and Winegard, W.C., J. Inst of Metals, 93 (1964-65) 457.

18. Haworth, C.W., and Whelan, R.P., J. Aust. Inst. of Metals, 10 (1965), 104.

19. Swalin, R.A., Acta. Met. 7 (1959), 736.

20. Ma, C.H., and Swalin, R.A., Acta Met. 8 (1960), 388.

21. Rumball, W.M., and Kondic, V., Iron and Steel Institute (London) Publication No. 110, (1967), 149.

22. Rumball, W.M., and Kondic, V., Trans. AIME 239 (1967), 586.

23. Chadwick, G.A., Iron and Steel Institute (London), Publication No. 110 (1967), 138.

24. Hunt, J.D. and Chilton, J.P., J. of Inst. of Metals, 91 (1962-63), 338.

25. Day, M.G., and Hellawell, A., J. Aust. Inst. of Metals, 9 (1964), 213.

26. Hunt, J.D., J. Inst. of Metals, 94 (1966), 125.

27. Cooksey, D.J.S., Day, M.G., and Hellawell, A., J. Phys. Chem. of Solids Suppl. No. 1 (1967), 151.

28. Moore, A., and Elliott, R., J. Inst. of Metals, 96 (1968), 62.

29. Davies, V.de.L., J. Inst. of Metals, 92 (1963-64), 127.

30. Yue, A.S., Trans. AIME 227 (1963).

31. Chadwick, G.A., J. Inst. of Metals, 91 (1962-63), 169.

32. Yue, A.S., Trans. AIME 224 (1962), 1010.

33. Pomboy, F.D., Hertzberg, R.W., and Bond, J.A., Trans. AIME 233 (1965), 334.

34. Jackson, K.A., and Hunt, J.D., Trans. AIME 236 (1966), 1129.

35. Pidler, R.S., Spittle, J.A., Taylor, M.R. and Smith, R.W. Iron and Steel Institute (London) Publication No. 110 (1967), 173.

36. Hunt, J.D., J. Crystal Growth 3-4 (1968), 82.

37. Kerr, H.W. and Winegard, W.C., J. Metals, 18 (1966), 563.

38. Day, M.G., Iron and Steel Institute (London) Publication No. 110, (1967), 177.

39. Hunt, J.D. and Hurle, D.T.J., Trans. AIME, 242 (1968), 1043.

40. Hulme, K.F., and Mullin, J.B., J. Phys. Chem. of Solids, 17 (1960), 1.

41. Hurle, D.T.J., and Jakeman, E., J. Crystal Growth 3-4 (1968), 574.

42. Kerr, H.W., and Winegard V.C., Can. Met. Quar. 6 (1967), 55.

43. Miller, W.A., and Chadwick, G.A., Iron and Steel Institute (London) Publication No. 110 (1967), 49.

44. Whelan, E.P., and Hayworth, C.W., J. Aust. Inst of Metals 12, (1967), 77.

45. Gigliott, M.F.X., Powell, G.L.F., Jr., and Colligan, G.A., Met. Trans. 1(4) (1970), 1038.

46. Digger Thomas, G.Jr., and Tauber, R.N., J. Crystal Growth, 8(1) (1971), 132.

47. Southin, R.T., and Jones B.L., J. Aust. Inst. of Metals, 13(4) (1968), 203.

48. Tayler, M.R., Fidler R.S., and Smith, R.V., J. Crystal Growth, 3-4 (1968), 666.

49. Fidler, R.S., Tayler, M.R., and Smith R.V., Can. Met. Quart. 8(4) (December 1969), 319.

50. Kerr, H.W., and Winegard W.C., Can. Met. Quart. 6(1), (1967),67.

51. Day, M.G., and Hellawell, A., Proc. Roy. Soc. A, 305 (1968), 473.

52. Hellawell, A., Progress in Material Science, Vol. 15, No.1(1970).

53. Pfann, W.G., Zone Melting, John Wiley and Sons.

54. Parr, N.L., Zone Refining and Allied Technique.

55. Pfann, W.G., Scientific American, (Dec. 1967), 63.

56. Lawley, A., Technique of Material Preparation and Handling, Vol. 1, Part 2, p. 845.

57. Aleksandrov, B.N., and Verkin, B.I., Physics of Metals and Metallography, Vol. 9, No. 3, (1960), 74.

58. Wernick, J.H. and Thomas, E.E., Trans. AIME, 218 (1960), 763.

59. Wernick, J.H. Benson, K.E. and Dorsi, D., Trans. AIME 209 (1957), 996.

60. Mullins, W.W., Acta Met. 4 (1956), 425.

61. Schaefer, R., Nakada, Y., and Ramaswami, B., Trans. AIME, 230 (1964), 605.

62. Wernick, J.H., Dorsi, D., and Byrnes, J.P., J. Electro Chemical Society, 106 (1959), 246.

63. Demmler, Jr. A.W., Trans. AIME, 206 (1956), 958.

64. Aleksandrov, B.N., Physics of Metals and Metallography 9 No.1, (1960), 46.

65. Tanenbaum, M., Gross, A.J., and Pfann, W.G., Trans. AIME, 200, (1954), 762.

66. Tiller, W.A., and Rutter, J.W., Canadian, J. Physics, 34 (1956), 96.

67. Yue, A.S., and Clark, J.B., Trans. AIME, 221 (1961), 383.

68. Hansen, M., McGraw Hill Book Co. Ltd., (1958).

69. Billig, E., J. Inst. Metals, 83 (1954-55), 53.

70. Bolling, G.E., Tiller, W.A., and Rutter, J.W., Canad. J. Phys. 34 (1956), 234.

71. Davydov, A.A., and Maslov, V.N., Sov. Phys. Crystallog. 9 (1965), 393.

ME-1972-M-KUM-EFF